UNCLASSIFIED

AD_____

Report Number 1

Dynamic Analysis of the Graze Module of the Hi-Performance Point Detonating Fuge (U)

Final Report

Dr. Joseph F. Shelley

July, 1971

Picatinny Arsenal

Dover, New Jersey 07801

Edutronics Analysis, Inc.
2294 Edgewood Terrace
Scotch Plains, New Jersey 07076

CONTRACT NO. DAAA 21-71-C-0066

Distribution of this document is unlimited

Destroy thi report when no longer needed
Do not return it to the originator.

The findings in this report are not to be construed as an official Department of the Army position.

UNCLASSIFIED

UNCLASSIFIED

DOCUMENT CONTROL DATA - R & D

1. Originating Activity Edutronics Analysis, Inc. Scotch Plains, New Jersey	2a. Unclassified 2b.

3. Report Title: DYNAMIC ANALYSIS OF THE GRAZE MODULE OF THE HI-PERFORMANCE POINT DETONATING FUZE

4. Descriptive Notes: Final Report September 1970 - December 1970

5. Author: Shelley, Joseph F.

6. Report Date: July, 1971	7a. Total Pgs: 102	7b. Refs.: 0
8a: Contract DAAA 21-71-C-0066	9a. Originator's Report No. Technical Report 1	
	9b. Other Report No(s).: None	

10. Distribution Statement: Distribution of this document is unlimited

11. Supplementary Notes	12. Sponsering Military Activity Picatinny Arsenal, Dover, N. J.

13. Abstract:

The equations of motion are presented for the inertia weight, firing pin and detent balls of the graze module of the high performance point detonating fuze. These equations are all in terms of the generalized graze forcing functions. The equations are also presented for the case where the graze forcing function-time plot is assumed to have a triangular shape. The criteria are established for the minimum values of forcing functions required to activate the graze module. All differential and constraint equations are presented in numerical form, but no numerical results are obtained. The numerical constants used are for the 105mm Howitzer Shell, M1.

UNCLASSIFIED

DD FORM 1473

REPORT NUMBER 1

Dynamic Analysis of the Graze Module of the Hi-Performance Point Detonating Fuze (U)

FINAL REPORT

Dr. Joseph F. Shelley

June, 1971

PICATINNY ARSENAL
Dover, New Jersey 07801

Edutronics Analysis, Inc.
2294 Edgewood Terrace
Scotch Plains, New Jersey 07076

CONTRACT NO. DAAA21-71-C-0066

ABSTRACT

The equations of motion are presented for the inertia weight, firing pin and detent balls of the graze module of the high performance point detonating fuze. These equations are all in terms of the generalized graze forcing functions. The equations are also presented for the case where the graze forcing functions-time plot is assumed to have a triangular shape. The criteria are established for the minimum values of forcing functions required to activate the graze module. All differential and constraint equations are presented in numerical form, but no numerical results are obtained. The numerical constants used are for the 105mm Howitzer Shell,M1.

TABLE OF CONTENTS

APPENDICES

ILLUSTRATIONS

Figure

TABLES

APPENDIX ILLUSTRATIONS

Figure

1. INTRODUCTION

The Fuze Research and Engineering Division, AED, at Picatinny Arsenal presently has an ongoing development program for the Hi-Performance fuze. One element of this program is the response of the graze module of the fuze to various forcing functions acting on the shell casing. The senior scientist of Edutronics Analysis, Inc., Dr. Joseph F. Shelley, had formerly been a consultant to the Fuze Research and Engineering Division, Picatinny Arsenal, through the Army Research Organization at Duke University. In this capacity he performed a preliminary analysis[1] of the operation of the graze module. The results of this analysis identified the conditions which are required to obtain dynamic response of the graze module under the application of the grazing forces. This study indicated that a more detailed analysis of the motion of the several elements of the graze module, with various values of forcing functions, was required in order to define the dynamic force-motion history of this fuze mechanism.

The present Picatinny Arsenal design of the graze module of the Hi-Performance fuze is a purely mechanical device. Its essential elements are a weight which is concentric with the long axis of the shell, and which has an inclined face, eight steel balls which are equally spaced about the long axis of the shell, three springs which hold the weight in a rearward position against the balls, and a housing which contains the entire assembly.

In the case of normal impact of a shell on a terrain the firing function is straightforward, since the force of the decelerating shell is available to activate the central firing plunger in the nose of the shell. When the shell grazes the terrain, however, there will be some angle of graze below which the central firing plunger will not be activated. The graze module is designed to effect the firing function in this case

When the shell grazes the terrain, the resulting lateral acceleration field acting on the graze module has the effect of forcing several of the steel balls against the inclined face of the weight. The weight then moves forward towards the nose of the shell. As this weight moves forward, two detent lock-

---

(1) Preliminary analysis of graze module of high performance PD Fuze assembly - Dr. Joseph F. Shelley, January, 1970, Unpublished Picatinny Arsenal Report.

ing balls are released and a spring loaded, internal firing pin is free to close.

In order to evaluate the effectiveness of the graze module, both as an individual mechanism and as an element of the fuze system, the following information is required.

1. The minimum magnitudes of the external graze forcing functions on the shell casing which will cause the device to function.
2. The time for the weight to move forward sufficiently to release the two detent balls.
3. The time, after the release of the two detent balls for the internal firing pin to move to the closed position with sufficient energy to activate the initiator.

2. OPERATION OF THE GRAZE MODULE

Figures 1 and 2 show the elements of the graze module. The vertical center axis in Figure 1 is the shell longitudinal center axis. In the inactive position, the 8 steel balls, A, and the 4 detent locks, C, are in the position shown. The 3 creep springs, F, force the inertia weight, B, downward at all times. When the shell leaves the barrel, the spin velocity causes the detent locks, C, to assume maximum outboard positions, so that the inertia weight is free to move upward. When the shell grazes on the terrain , several of the steel balls, A, are forced radially inward and the inertia weight, B, is forced upward. When this inertia weight has moved upward by a sufficient amount, the two firing pin detent balls, D, move radially outward. After sufficient movement of these two balls, the firing pin, E, moves downward under the influence of the firing pin spring, G. When the firing pin assumes its maximum downward position, the firing process is initiated.

3. ASSUMPTIONS

The assumptions used in the present study are listed below.

a. The present analysis is for the case where the graze module is in a partially static condition. As the shell grazes the terrain , there will be a graze force acting on it for a short duration. Due to the spin of the shell, there will be a continually varying position of any graze ball with respect to the line of action of this force. It will be assumed in this first analysis, subject to confirmation, that the time for the total firing process to occur is less than the time for any ball to occupy a successive position. The effect of this assumption is to reduce the problem to the situation de-

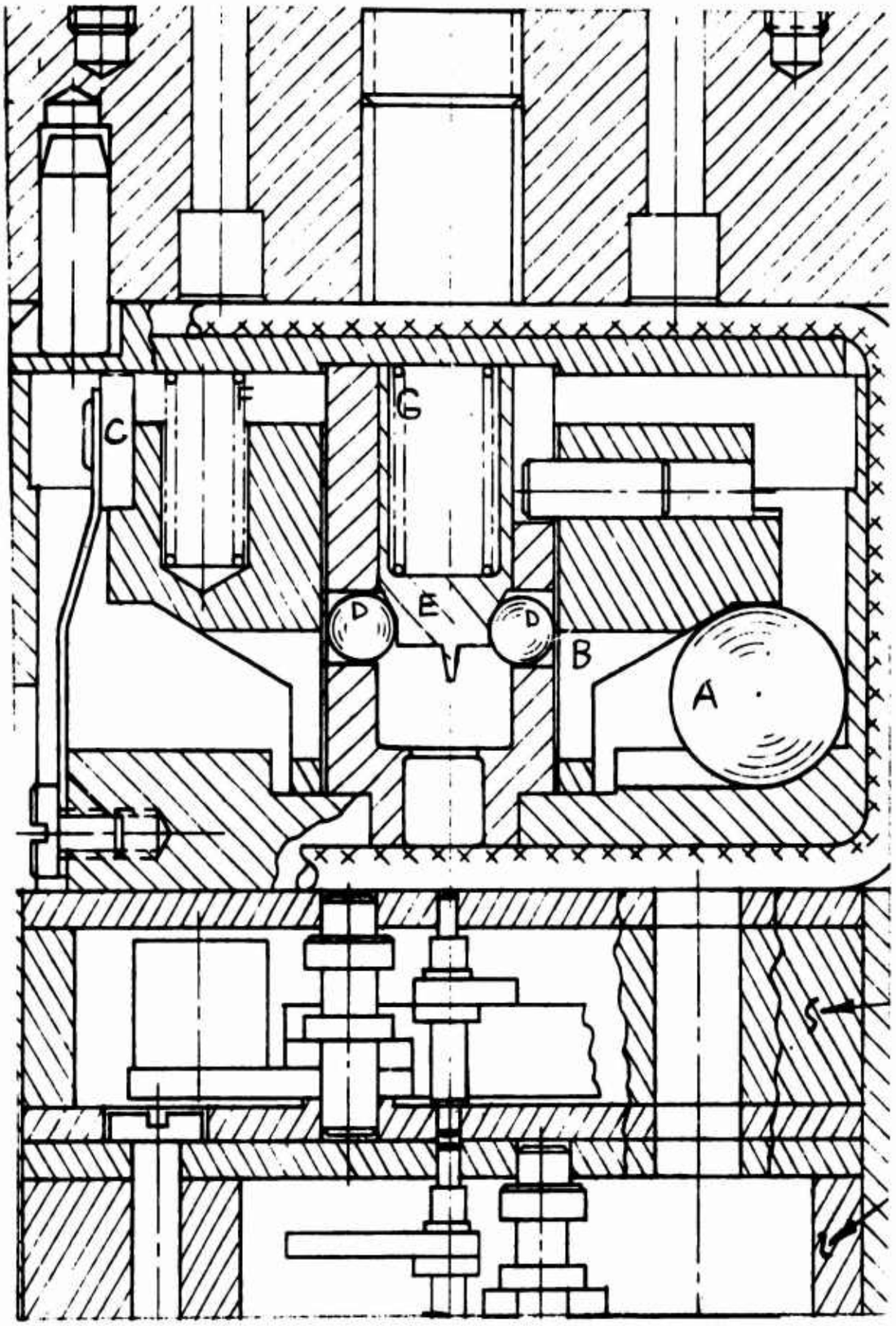

Figure 1 - Graze Module - Side View

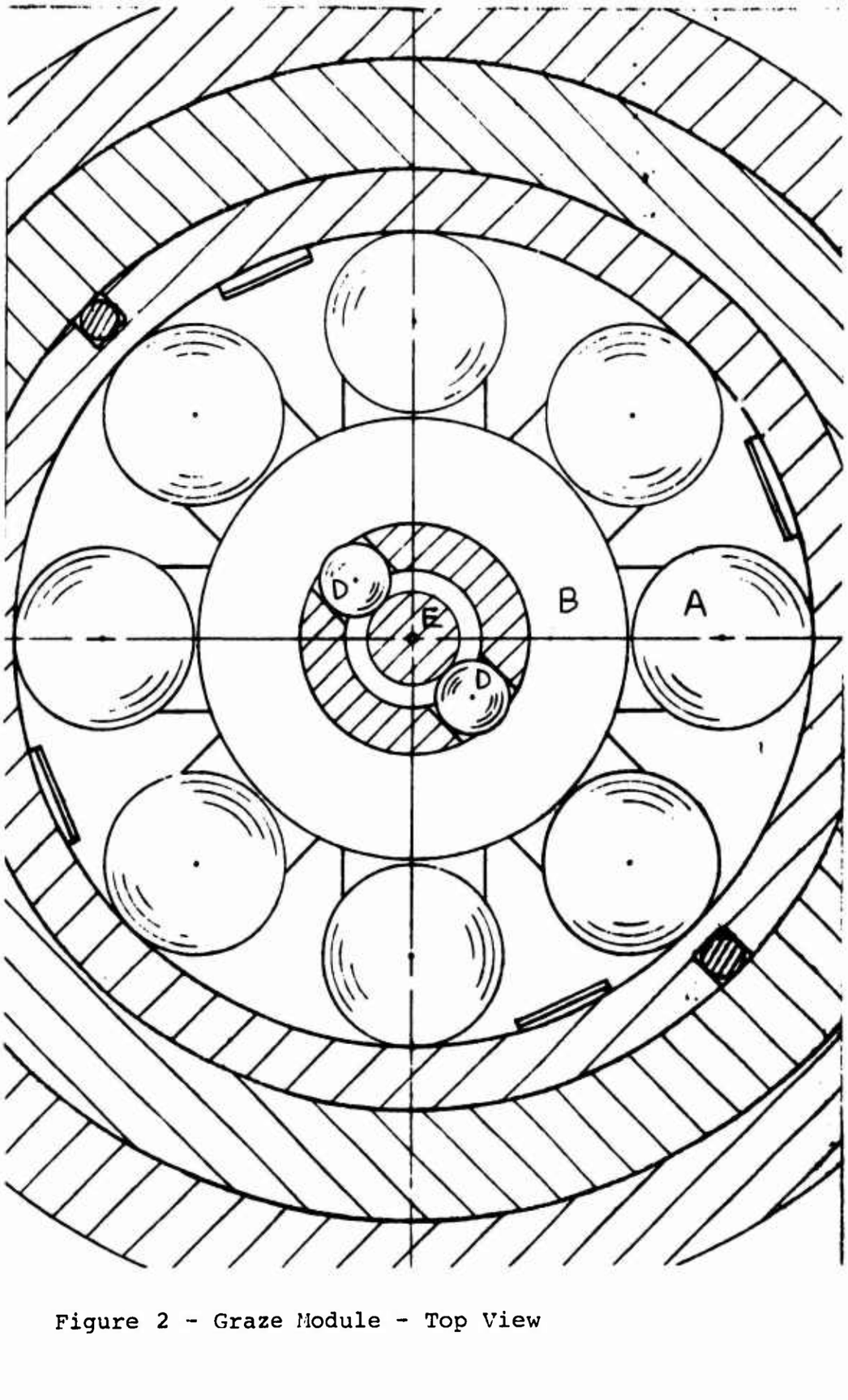

Figure 2 - Graze Module - Top View

picted in Figure 3. In this Figure, a_T is the total

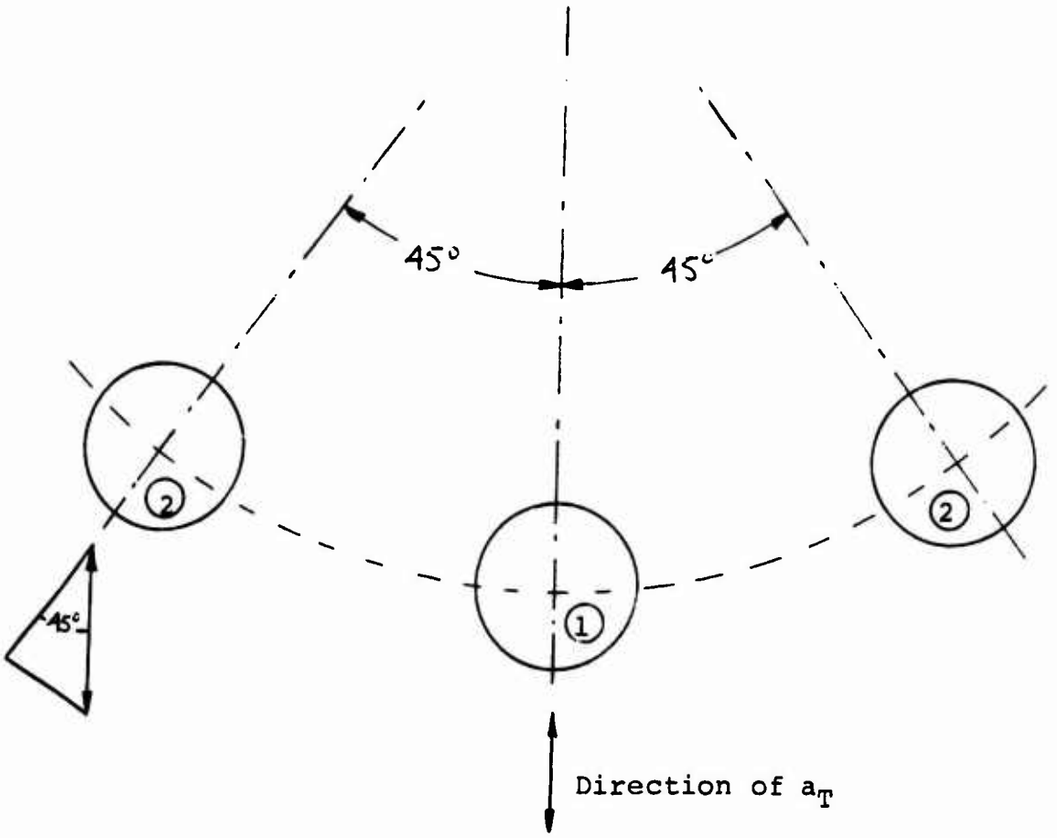

Figure 3 - Graze Ball Orientation

lateral acceleration of the graze module housing. Balls 1 and 2 will be referred to as the primary and secondary balls, respectively. The assumption implied by Figure 3 is that the present study considers the case where the radial position vector of ball 1 is collinear with the direction of a_T and that these directions are constant with respect to each other.

b. All friction forces are neglected except the friction forces between:
    1. the inertia weight and the firing pin housing of the graze module.
    2. the firing pin and the firing pin housing of graze module.

c. The coefficient of friction between all sliding parts is constant.

d. The spin velocity of the shell is constant, and the other components of rotation of the shell are small.

e. During graze the shell moves in a plane which is normal to the graze terrain , and the shell remains at a constant angle with respect to this terrain.

f. The graze module activating balls translate only in a plane through the center axis of the graze module, and thus the tendency of the graze balls to move circumferentially out of their radial groove is neglected.

g. The direction of a_T is collinear with the line joining the two detent balls. This orientation is also assumed to be constant throughout graze, for the reasons given in assumption a.

h. The dimension C_2 is constant, and the details of this conclusion are recorded in Appendix B.

i. The graze force P acts at the tip of the ogive shell nose.

j. The mass moment of inertia of the firing pin, about an axis through its center of mass and normal to the longitudinal axis of the shell, is negligible.

k. The firing pin only moves forward with respect to the graze module housing.

l. The firing pin spring is a massless element with a constant spring rate.

m. The forcing function for one case is assumed to have a triangular shape, and for this case the equations of motion are expressed in numerical form.

n. The centripetal acceleration of the graze module, with respect to an axis through the center of mass of the shell and normal to the center axis of the shell, is negligible.

4. ACCELERATION FIELD OF THE GRAZE MODULE DUE TO THE SHELL FORCING FUNCTIONS

The typical shell is shown in Figure 4. The dimensions d and ℓ are peculiar

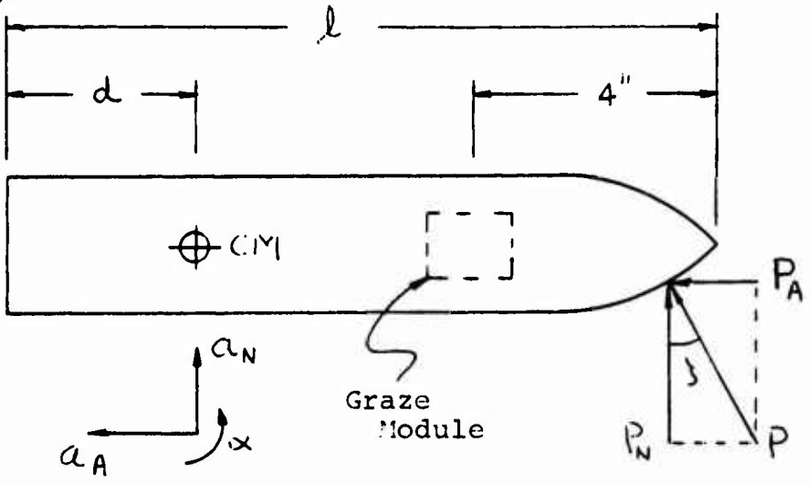

Figure 4 - Shell and Graze Force Relationships

to a given shell. a_A, a_N and α are components of acceleration of the center of mass, CM, of the shell. P_A and P_N are components of the graze force $P(t)$ and ζ is the graze angle. The graze module is at a constant distance from the nose for all shells. The graze force P is some complicated function of time, and it will be carried through the present derivation in symbolic form. The equations of motion of the shell are

$$P_N = m a_N \tag{4-1}$$

$$P_A = m a_A \tag{4-2}$$

$$P_N (\ell - d) = I_{CM} \alpha \tag{4-3}$$

Where m is the mass of the shell, I_{CM} is the moment of inertia with respect to the CM, a_N and a_A are accelerations with senses as shown in Figure 4, and α is the angular acceleration of the shell.

The total lateral acceleration a_T of the graze module is

$$a_T = a_N + (\ell - d - 4)\alpha \tag{4-4}$$

$$a_T = \frac{P_N}{m} + (\ell - d - 4) P_N \frac{(\ell - d)}{I_{CM}} \tag{4-5}$$

Using

$$\overline{I}_{CM} = m K_{CM}^2 \tag{4-6}$$

where K_{CM} is the radius of gyration,

$$a_T = \frac{P_N}{m}\left[1 + \frac{(\ell-d)(\ell-d-4)}{K_{CM}^2}\right] \tag{4-7}$$

Equation (4-7) may be used directly to find a_T, when P_N is known.

From Equation (4-7)

$$a_T \sim P_N \tag{4-8}$$

and from Equation (4-2),

$$a_A \sim P_A \tag{4-9}$$

P_A and P_N are components of the same force, so that

$$P_A \sim P_N \tag{4-10}$$

and therefore

$$a_A \sim P_N \tag{4-11}$$

Finally, from Equation (4-3)

$$\alpha \sim P_N \tag{4-12}$$

Consideration of the above results now leads to the conclusion

$$a_A, \alpha \sim a_T \tag{4-13}$$

or

$$a_A = K_1 a_T \tag{4-14}$$

$$\alpha = K_2 a_T \tag{4-15}$$

where K_1 and K_2 are known constants. These results will subsequently be used to express the right hand sides of the equations of motion in terms of a_T only.

For the purpose of the present analysis, the graze module will be assumed to experience acceleration components which are oriented as in Figure 5.

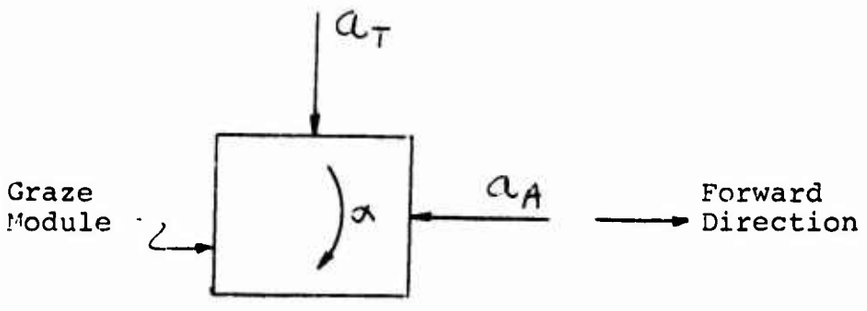

*

Figure 5 - Acceleration Components Acting on Graze Module

5. ABSOLUTE ACCELERATION OF THE GRAZE MODULE ACTIVATING BALLS

To obtain the accelerations of the balls and of the inertia weight, a secondary coordinate system will be used. Figure 6 shows the general system.

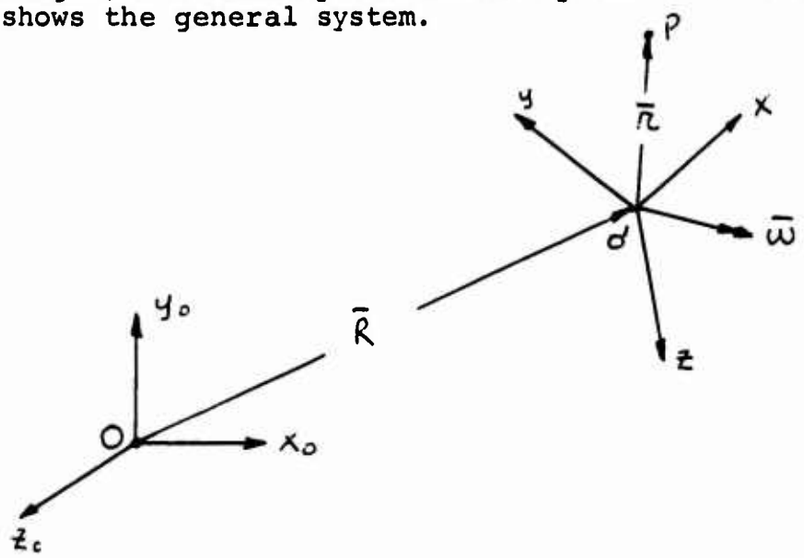

Figure 6 - Coordinate Axes Orientation

x_o, y_o, z_o are inertial coordinates, and the x, y, z coordinates rotate with absolute angular velocity $\bar{\omega}$. The absolute acceleration $\bar{a}_o$ of point P is then

$$\bar{a}_o = \ddot{\bar{R}} + \ddot{\bar{r}}_r + \frac{d\bar{\omega}}{dt} \times \bar{r} + 2\bar{\omega} \times \dot{\bar{r}}_r + \bar{\omega} \times (\bar{\omega} \times \bar{r}) \quad (5\text{-}1)$$

Each of these terms will now be identified. $\ddot{\bar{R}}$ is the absolute acceleration of O', the origin of the secondary coordinate system.

*The senses of certain components, for convenience, are different from those shown in Figure 4

$\ddot{\bar{r}}_R = \bar{i}\ddot{x} + \bar{j}\ddot{y} + \bar{k}\ddot{z}$, where $\bar{i}, \bar{j}, \bar{k}$ are unit vectors in the x, y, z coordinate system, is the relative acceleration, measured in the x, y, z frame of reference.

$\dot{\bar{r}}_R = \bar{i}\dot{x} + \bar{j}\dot{y} + \bar{k}\dot{z}$ is the relative velocity, measured in the x, y, z frame of reference.

$\bar{r} = \bar{i}x + \bar{j}y + \bar{k}z$ is the position vector, in the x, y, z system, of the point P.

$d\bar{\omega}/dt$ is the time rate of change of $\bar{\omega}$

$\frac{d\bar{\omega}}{dt} \times \bar{r}$ is the tangential acceleration effect

$2\bar{\omega} \times \dot{\bar{r}}_R$ is the coriolis acceleration

$\bar{\omega} \times (\bar{\omega} \times \bar{r})$ is the centripetal acceleration.

From Figure 3, the primary activating ball, Ball 1, lies on the line of action of the graze module lateral acceleration a_T. The secondary balls, Balls 2, are located symmetrically with respect to Ball 1. Equation (5-1) will now be used to obtain the absolute accelerations of Balls 1 and 2.

The secondary x, y, z coordinate axes are attached to the graze module housing. The x axis passes through the center of the primary Ball 1 and the y axis is collinear with the axis of the inertia weight. The orientation is shown in Figure 7. These coordinates will rotate with the graze module and thus possesses the spin velocity of the shell. For this orientation of a_T the primary ball is forced radially inward and it tends to move the inertia weight forward.

The absolute acceleration $\bar{a}_{o,1}$ of the primary ball will now be obtained. The rotation $\bar{\omega}$ is

$$\bar{\omega} = \bar{j}\,\omega_y \qquad (5\text{-}2)$$

since $\omega_x \doteq 0$ and $\omega_z \doteq 0$. ω_y, the spin velocity, is assumed to be constant. The position vector $\bar{r}$ of Ball 1 is

$$\bar{r} = \bar{i}X \qquad (5\text{-}3)$$

so that X locates the center of Ball 1.

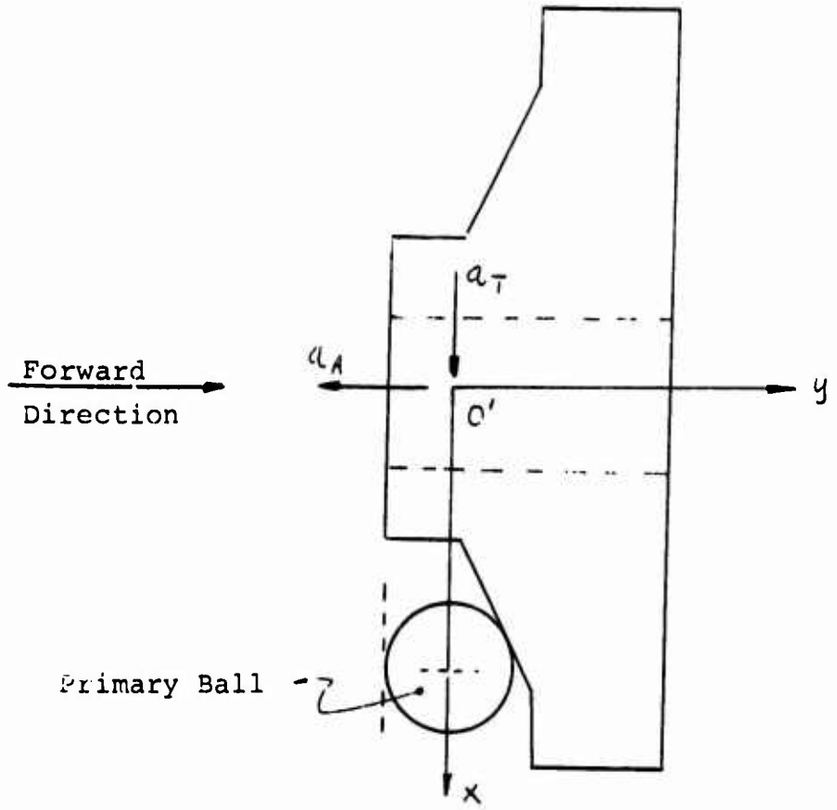

Figure 7 - Coordinate Axes Orientation on Graze Module

The several other terms now appear as

$$\ddot{\bar{R}} = \bar{c}(a_T) + \bar{j}(-a_A) \tag{5-4}$$

$$\dot{\bar{r}}_r = \bar{c}\,\dot{x} \tag{5-5}$$

$$\ddot{\bar{r}}_r = \bar{c}\,\ddot{x} \tag{5-6}$$

$$\frac{d\bar{\omega}}{dt} \times \bar{r} = \bar{0} \times \bar{r} = 0 \tag{5-7}$$

$$\bar{\omega} \times \dot{\bar{r}}_R = \begin{vmatrix} \bar{\imath} & \bar{\jmath} & \bar{k} \\ 0 & 2\omega_y & 0 \\ \dot{x} & 0 & 0 \end{vmatrix} = \bar{k}(-2\omega_y \dot{x}) \qquad (5\text{-}8)$$

$$\bar{\omega} \times \bar{r} = \begin{vmatrix} \bar{\imath} & \bar{\jmath} & \bar{k} \\ 0 & \omega_y & 0 \\ x & 0 & 0 \end{vmatrix} = \bar{k}(-x\omega_y) \qquad (5\text{-}9)$$

$$\bar{\omega} \times (\bar{\omega} \times \bar{r}) = \begin{vmatrix} \bar{\imath} & \bar{\jmath} & \bar{k} \\ 0 & \omega_y & 0 \\ 0 & 0 & -x\omega_y \end{vmatrix} = \bar{\imath}(-x\omega_y^2) \qquad (5\text{-}10)$$

The final result for the absolute acceleration is then

$$\bar{a}_{0,1} = \bar{\imath}\left[\ddot{x} - x\omega_y^2 + a_T\right] + \bar{\jmath}\left[-a_A\right] + \bar{k}\left[-2\omega_y \dot{x}\right] \qquad (5\text{-}11)$$

Figure 8 shows the primary ball 1 and the two secondary balls 2. The acceleration field a_T was assumed to be uniform along a direction normal to the shell axis and have a constant direction with respect to the position of the three balls. Thus, if Ball 1 experiences a_T, then Balls 2 experience a corresponding acceleration

$$a_T \cos 45^\circ = 0.707\, a_T$$

The acceleration of Balls 2, $\bar{a}_{0,2}$, would then be given by Equation (5-11) with a_T replaced by $0.707\, a_T$.

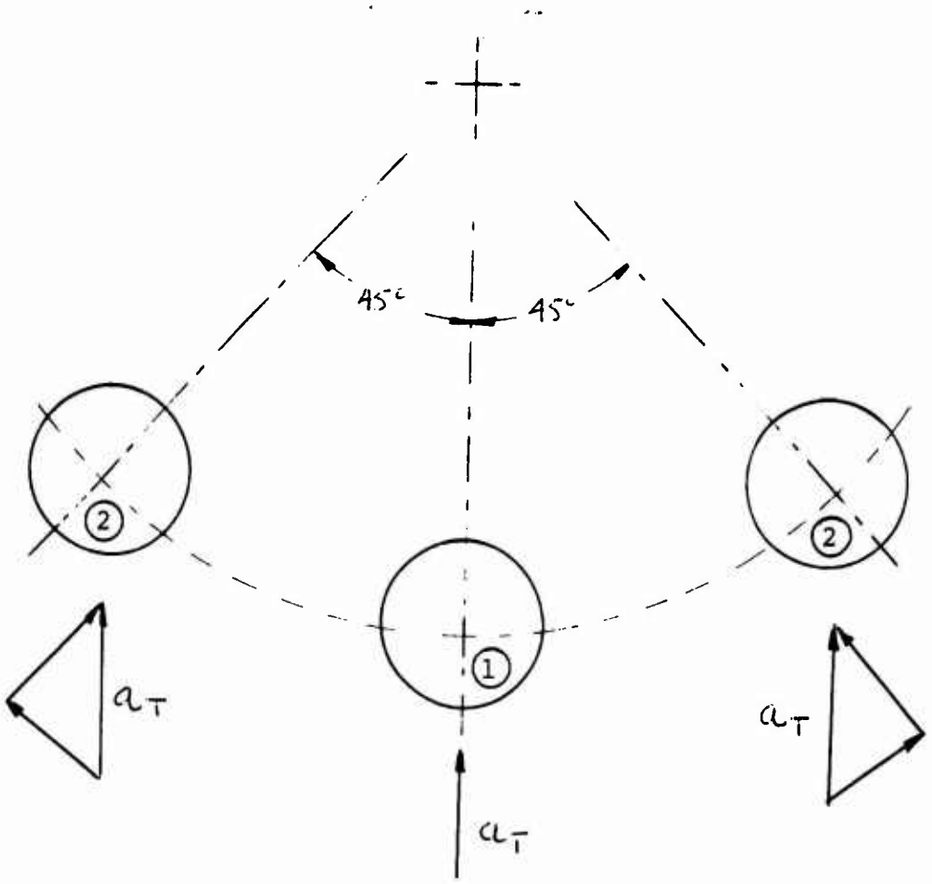

Figure 8 - Acceleration Components Acting on Graze Balls

For this case, the secondary X axis would pass through Ball 2.

It may be seen from Equation (5-11) that there will be an inertia force on the balls in the Z direction, of magnitude $2m_3\omega_y\dot{X}$, where m_3 is the mass of the activating ball. This force will tend to displace the balls in a circumferential direction. This effect is assumed to be small compared to the other forces on the ball and accounts, in retrospect, for assumption f.

6. DYNAMIC EQUILIBRIUM REQUIREMENTS OF THE GRAZE MODULE ACTIVATING BALLS

The free body diagram of the primary ball 1, together with the inertia forces, is shown in Figure 9. The ramp angle of the inertia weight is θ.

$F_{6,1}$ is the reaction force on Ball 1 by the floor of the graze module, and $F_{1,1}$ is the normal reaction force between Ball 1 and the inertia weight. The friction forces induced by $F_{6,1}$ and $F_{1,1}$ are zero, in view of assumption b. These effects could be included in a more refined study.

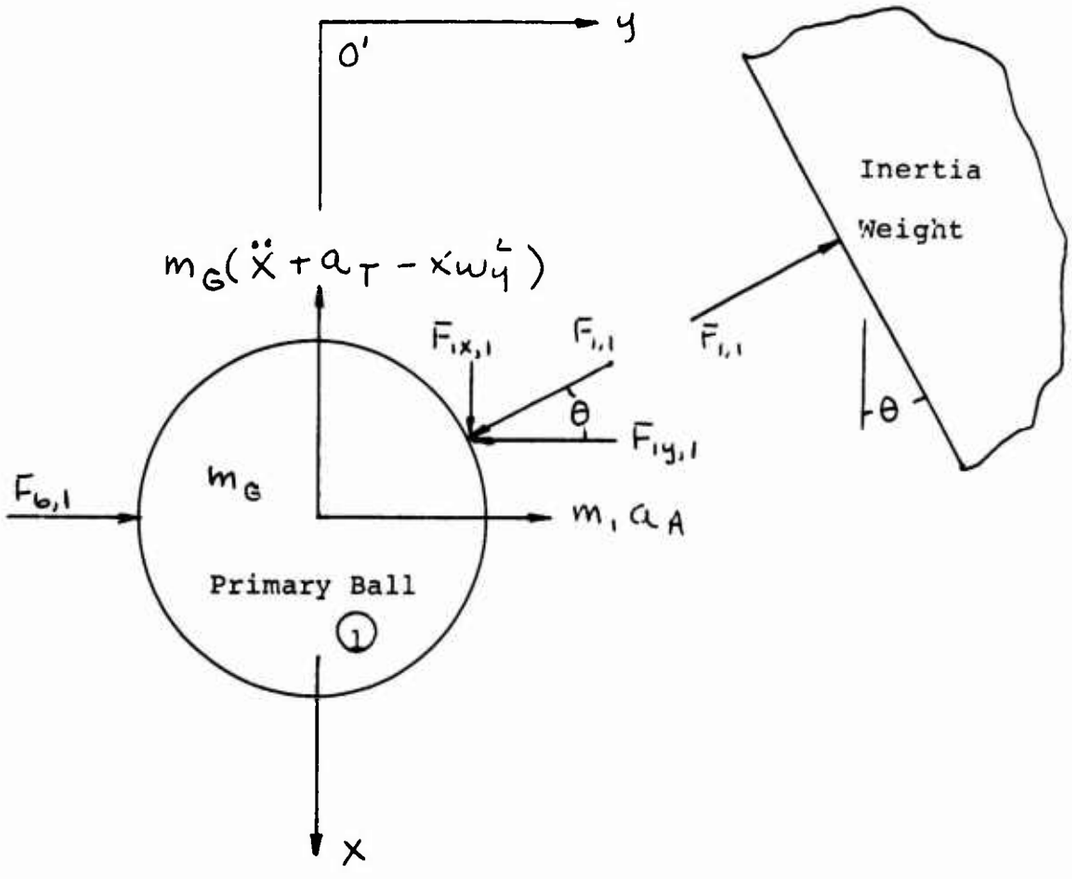

Figure 9 - Free Body Diagram of Primary Ball

The components of $F_{1,1}$ are related by

$$F_{1x,1} = F_{1y,1} \tan\theta \tag{6-1}$$

A necessary constraint condition is that

$$F_{1,1} \geq 0 \tag{6-2}$$

$$F_{6,1} \geq 0 \tag{6-3}$$

since these forces are compressive contact forces.

Since Figure 9 is a concurrent force system, the equilibrium requirements are

$$F_{1x,1} = m_G(\ddot{x} + a_T - x\omega_y^2) \quad (6\text{-}4)$$

The constraint equation is

$$x \leq x_o$$

where x_o is defined on page 88.

$$F_{1y,1} = m_G a_A + F_{6,1} \quad (6\text{-}5)$$

$F_{1x,1}$ is eliminated between Equations (6-1) and (6-4), with the result

$$F_{1y,1} = m_G \cot\theta(\ddot{x} + a_T - x\omega_y^2) \quad (6\text{-}6)$$

Equations (6-5) and (6-6) are now combined to find $F_{6,1}$ and

$$F_{6,1} = m_G \cot\theta(\ddot{x} + a_T - x\omega_y^2) - m_G a_A \quad (6\text{-}7)$$

The above equation is obviously true only for $F_{6,1} > 0$.

The opening effect of the ball on the inertia weight is indicated by the magnitude of $F_{1y,1}$. From Equation (6-6), as the ball moves inward $\ddot{x} < 0$ and x decreases and only the term a_T is always positive.

Since the desired final result of this study is an equation of motion of the inertia weight in terms of y, all x quantities and their derivatives will be expressed in terms of y. Figure 10 shows the kinematic relationships as the ball moves inward.

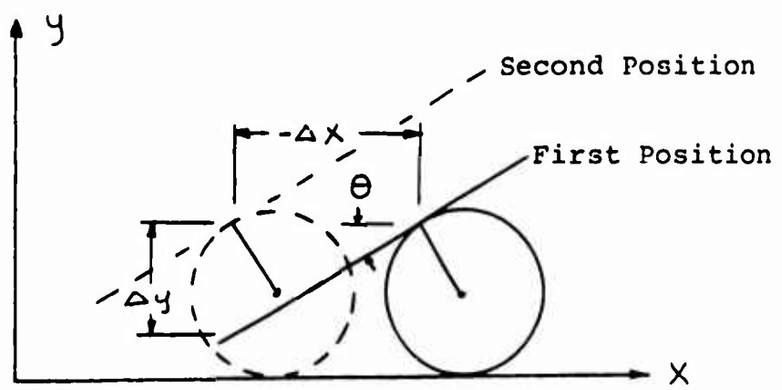

Figure 10 - Kinematic Relationship Between Graze Ball and Inertia Weight

$$\tan\theta = \frac{\Delta y}{\Delta x} \tag{6-8}$$

$$\Delta y = -\Delta x \tan\theta \tag{6-9}$$

$$\frac{\Delta y}{\Delta t} = \frac{-\Delta x}{\Delta t}\tan\theta \tag{6-10}$$

$$\ddot{y} = -\ddot{x}\tan\theta \tag{6-11}$$

$$\ddot{x} = -\ddot{y}\cot\theta \tag{6-12}$$

X and y displacements are related by an equation of the form

$$X = C_\theta y + C_q \tag{6-13}$$

where C_θ and C_q are constants to be chosen later. Equation (6-6) now appears as

$$F_{1y,1} = m_G \cot\theta\left[-\ddot{y}\cot\theta + a_T - (C_\theta y + C_q)\omega_y^2\right] \tag{6-14}$$

The y components of the reaction forces on Balls 2, designated by $F_{1y,2}$, are then

$$F_{1y,2} = m_G \cot\theta\left[-\ddot{y}\cot\theta + 0.707 a_T - (C_\theta y + C_q)\omega_y^2\right] \tag{6-15}$$

Each of the remaining five balls will exert a direct axial force $F_{1y,3}$, on the inertia weight of magnitude

$$F_{1y,3} = m_G a_A \tag{6-16}$$

and acting in the positive y sense.

The total force $F_{y,TOT.}$ of the balls on the inertia weight, acting in the positive y sense, is then

$$F_{y,TOT.} = F_{1y,1} + 2F_{1y,2} + 5F_{1y,3} \tag{6-17}$$

$$F_{y,TOT.} = m_G \cot\theta\left[-\ddot{y}\cot\theta + a_T - (C_\theta y + C_q)\omega_y^2\right]$$

$$+ m_G \cot\theta\left[-\ddot{y}\cot\theta + 0.707 a_T - (C_\theta y + C_q)\omega_y^2\right]$$

$$+ 5 m_G a_A \qquad (6\text{-}18)$$

$$F_{y,TOT.} = m_G \left\{ \cot\theta \left[-3\ddot{y} \cot\epsilon + 2.41 a_T - 3(C_8 y \right. \right.$$

$$\left. \left. + C_9) \omega_y^2 \right] + 5 a_A \right\} \qquad (6\text{-}19)$$

The free body diagram of the secondary balls 2 is shown in Figure 11. The equilibrium equations for balls 2 are

$$F_{1y,2} = F_{6,2} + m_G a_A \qquad (6\text{-}20)$$

$$F_{1x,2} = F_{1y,2} \tan\theta = m_G \left[0.707 a_T - \ddot{y} \cot\theta - (C_8 y + C_9) \omega_y^2 \right] \qquad (6\text{-}21)$$

Each of balls 2 exert less axial force on the inertia weight because of the term $0.707 a_T$ in Equation (6-21) compared with the term a_T in Equation (6-14). A limiting condition for ball 2 is reached when

$$F_{6,2} \rightarrow 0 \qquad (6\text{-}22)$$

At this condition, following Equation (6-20),

$$F_{1y,2} \rightarrow m_G a_A \qquad (6\text{-}23)$$

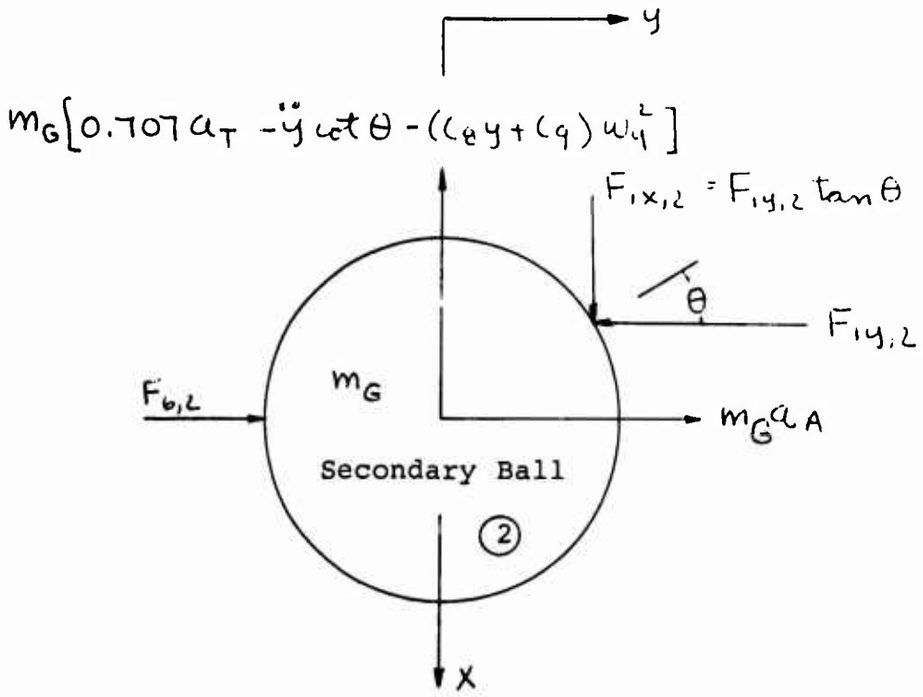

Figure 11 - Free Body Diagram of Secondary Ball

The graze forcing functions are applied to the shell at $t = 0^+$. If t_o is the time corresponding to Equation (6-23), then Equation (6-21) reduces to

$$\left\{ m_G a_A \tan\theta = m_G [0.707 a_T - \ddot{y} \cot\theta - (C_8 y + C_9) w_4^2] \right\}_{t=t_o} \quad (6\text{-}24)$$

or

$$\left\{ \ddot{y} = \tan\theta [0.707 a_T - (C_8 y + C_9) w_4^2 - a_A \tan\theta] \right\}_{t=t_o} \quad (6\text{-}25)$$

$$\Big\} \ddot{y} + C_8 y \dot{y}^2 \tan\theta = \tan\theta \Big[0.707 a_T - C_9 \omega_y^2 - C_H \tan\theta \Big] \Big\}_{t=t_o} \qquad (6\text{-}26)$$

With the numerical values in Appendix A, the above equation appears as

$$\Big\{ \ddot{y} - 2.68 \times 10^6 y = 0.408 a_T - 0.333 a_H - 1.6 \times 10^6 \Big\}_{t=t_o} \qquad (6\text{-}27)$$

After $y = y(t)$ is obtained, the time $t = t_o$ which satisfies Equation (6-27) may be obtained. The y component of force, $F_{y,TOT.}$, on the inertia weight for $t \geq t_o$ is then

$$F_{y,TOT.} = F_{IN,1} + 7 F_{IN,3} \qquad (6\text{-}28)$$

$$F_{y,TOT.} = m_G \cot\theta \Big[-\ddot{y} \cot\theta + a_T - (C_8 y + C_9) \omega_y^2 \Big]$$

$$+ 7 m_G a_H \qquad (6\text{-}29)$$

$$F_{y,TOT.} = m_G \Big\{ \cot\theta \Big[-\ddot{y} \cot\theta + a_T - (C_8 y + C_9) \omega_y^2 \Big]$$

$$+ 7 a_H \Big\} \qquad t \geq t_o \qquad (6\text{-}30)$$

where t_o is the time which satisfies Equation (6-27).

The term $7F_{1y,3}$ in Equation (6-28) reflects the direct axial effect of the balls which do not contribute wedging action on the inertia weight. The two possible regimes of motion will now be summarized.

Case I - For $0 \leq t \leq t_o$, the primary and secondary balls contribute wedging action and the remaining five balls contribute direct axial effect. Equation (6-19) expresses the axial force acting on the inertia weight.

Case II - For $t_o \leq t$, the primary ball only contributes wedging action while the remaining seven balls contribute direct axial effect. For this case, Equation (6-30) expresses the axial force on the inertia weight.

A continuous test of whether Case I or Case II operation occurs may be had by consideration of Equation (6-20). If $F_{6,2} > 0$, then the secondary balls contribute to the wedging effect of Balls 2 on the inertia weight. For this situation Equations (6-20) and (6-21) are valid. At times $t \geq t_o$, when $F_{6,2} = 0$, Equation (6-20) will still be valid, resulting in

$$F_{1y,2} = m_G a_A \tag{6-31}$$

However, Equation (6-21) will no longer be true, since the kinematic relationship between Balls 2 and the inertia weight, given by Equation (6-13), is no longer true.

$F_{1y,2}$ is eliminated between Equations (6-20) and (6-21), with the result

$$F_{6,2} = m_G \cot\theta \left[0.707 a_T - \ddot{y} \cot\theta - (C_8 y + C_9)\omega_y^2 - a_A \tan\theta \right] \tag{6-32}$$

In a similar fashion $F_{6,1}$, from Equation (6-7), (6-12) and (6-13) appears as

$$F_{6,1} = m_G \cot\theta \left[a_T - \ddot{y} \cot\theta - (C_8 y + C_9)\omega_y^2 - a_A \tan\theta \right] \tag{6-32a}$$

The condition $F_{6,2} > 0$ is thus, following Equation (6-32), equivalent to

$$\left[0.707\, a_T - \ddot{y}\cot\theta - (C_{\xi y} + C_{\eta})\,\omega_y^2 - a_A \tan\theta\right] \tag{6-33}$$

or

$$\left[-1.73\,\ddot{y} + 4.65\times 10^6\, y + 0.707\, a_T - a_A - 2.77\times 10^6\right] > 0 \tag{6-34}$$

Equation (6-34) may be used to determine whether Case I or Case II operation prevails, and the time t_o at which Case II operation commences is found from Equation (6-27).

7. ABSOLUTE ACCELERATION OF THE CENTER OF MASS OF THE INERTIA WEIGHT

With the secondary x, y, z coordinates positioned as described before, the absolute acceleration $\bar{a}_{o,I}$ of the center of mass of the inertia weight will now be obtained. The several terms needed in Equation (5-1) are

$$\bar{\omega} = \bar{j}\,\omega_y \tag{7-1}$$

$$\bar{r} = \bar{j}\, y \tag{7-2}$$

so that y is the position of the CM of the inertia weight.

$$\ddot{\bar{R}} = \bar{i}(a_T) + \bar{j}(-a_A) \tag{7-3}$$

$$\dot{\bar{r}}_R = \bar{j}\,\dot{y} \tag{7-4}$$

$$\ddot{\bar{r}}_R = \bar{j}\,\ddot{y} \tag{7-5}$$

$$\frac{d\bar{\omega}}{dt} \times \bar{r} = \bar{0} \times \bar{r} = 0 \tag{7-6}$$

$$2\bar{\omega} \times \dot{\bar{R}}_R = \begin{vmatrix} \bar{\imath} & \bar{\jmath} & \bar{k} \\ 0 & \omega_y & 0 \\ 0 & \dot{y} & 0 \end{vmatrix} = 0 \qquad (7\text{-}7)$$

$$\bar{\omega} \times \bar{R} = \begin{vmatrix} \bar{\imath} & \bar{\jmath} & \bar{k} \\ 0 & \omega_y & 0 \\ 0 & y & 0 \end{vmatrix} = 0 \qquad (7\text{-}8)$$

$$\bar{\omega} \times (\bar{\omega} \times \bar{R}) = 0 \qquad (7\text{-}9)$$

The absolute acceleration $\bar{a}_{0,I}$ is then

$$\bar{a}_{0,I} = \bar{\imath}(a_T) + \bar{\jmath}(-a_A + \ddot{y}) \qquad (7\text{-}10)$$

8. DYNAMIC EQUILIBRIUM REQUIREMENTS OF THE INERTIA WEIGHT

Figure 12 shows the applied and inertia forces acting on the inertia weight. These forces are identified below.

$F_{1,1}$, $F_{1x,1}$, $F_{1y,1}$; $F_{1,2}$, $F_{1x,2}$, $F_{1y,2}$ - reaction forces and components of Balls 1 and 2, as previously defined, on the inertia weight.

F_2, F_5 - Normal reactions of center rod on inertia weight

F_3, F_4 - Friction forces induced by F_2 and F_5

F_7 - Inertia force of inertia weight.

F_8 - Total force of three creep springs. K is the combined spring constant of the three springs

F_9 - Total initial force of 3 creep springs

$I_o\alpha$ - Inertia moment due to angular acceleration of shell. I_o is the mass moment of inertia about the CM.

The sense of the inertia force $m_I a_T$ which acts through the CM is obtained from the X component of Equation (7-10),

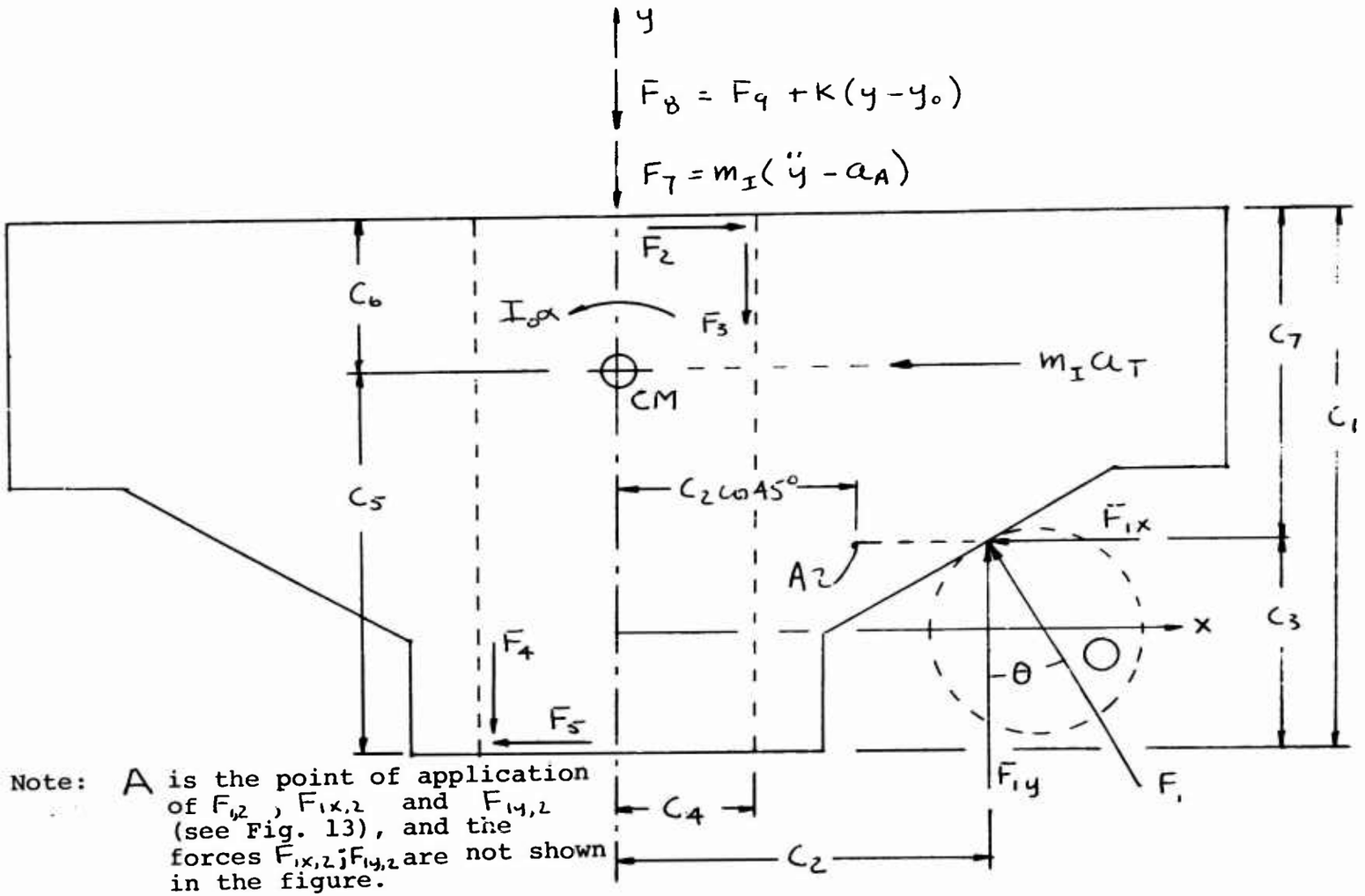

Note: A is the point of application of $F_{1,2}$, $F_{1x,2}$ and $F_{1y,2}$ (see Fig. 13), and the forces $F_{1x,2}$, $F_{1y,2}$ are not shown in the figure.

Figure 12 - Free Body Diagram of Inertia Weight

while the sense of the term $I_{o\alpha}$ is obtained from Figure 5.

The object of the subsequent analysis is to obtain the friction forces F_3 and F_4, so that a summation of forces in the y direction may be made. The moments will be summed about the CM. Figure 13 shows the configuration of the components of ball force which contribute to moment about the CM depicted in Figure 12. There will be a slight additional contribution to the sum of moments about the CM caused by the forces $F_{1y,3} = m_e a_A$, and these effects will be neglected.

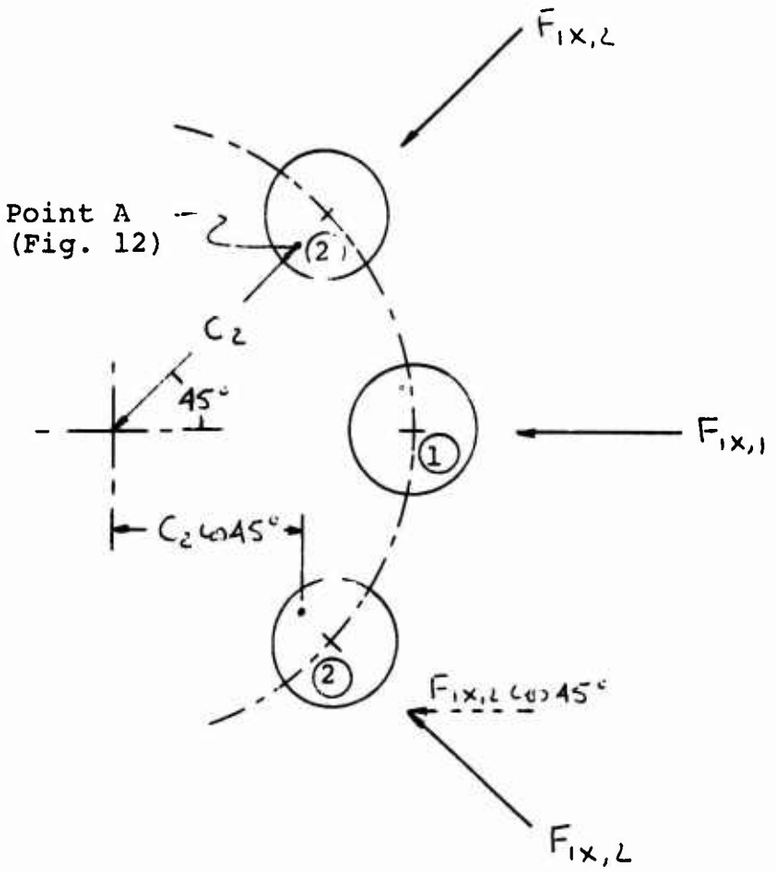

Figure 13 - Components of Force of Primary and Secondary Graze Balls

The equilibrium requirements, from Figure 12, are

$$\sum M_{CM} = 0 \qquad \text{(clockwise moments are positive)}$$

$$-I_o\alpha + F_2 C_6 + F_3 C_4 + F_{1x,1}(C_5 - C_3) - F_{1y,1} C_2$$

$$+ F_5 C_5 - F_4 C_4 + 2\{0.707 F_{1x,2}(C_5 - C_3)$$

$$- F_{1y,2}(0.707 C_2)\} = 0 \qquad (8\text{-}1)$$

$$\sum F_X = 0 \qquad \text{(Forces positive in positive X sense)}$$

$$F_2 - m_I a_T - F_{1x,1} - F_5 - 1.41 F_{1x,2} = 0 \qquad (8\text{-}2)$$

Motion of the inertia weight is assumed to be impending, so that

$$F_3 = \mu F_2 \qquad (8\text{-}3)$$

$$F_4 = \mu F_5 \qquad (8\text{-}4)$$

With the results

$$F_{1x,j} = F_{1y,j} \tan\theta \qquad j = 1,2 \qquad (8\text{-}5)$$

The normal reactions F_2 and F_5 are

$$F_2 = \frac{1}{C_1}\{I_o\alpha + (C_5 - \mu C_4) m_I a_T$$

$$+ [C_2 + (C_3 - \mu C_4)\tan\theta](F_{1y,1} + 1.41 F_{1y,2})\} \qquad (8\text{-}6)$$

$$F_5 = \frac{1}{C_1}\{I_o\alpha - (C_6 + \mu C_4) m a_T$$

$$+\left[C_2 - (C_7 + \mu C_4)\tan\theta\right](F_{1y,1} + 1.41\,F_{1y,2})\Big\} \quad (8\text{-}7)$$

The total friction force $F_{F,TOT.}$ is

$$F_{F,TOT.} = F_3 + F_4 = \mu(F_2 + F_5) \quad (8\text{-}8)$$

For equilibrium of the inertia weight in the y direction, from Figure 12, for

$$y \geq y_o$$

is

$$F_{1y,TOT.} - F_{F,TOT.} - m_I(\ddot{y} - a_A) - \left[F_9 + K(y - y_o)\right] = 0 \quad (8\text{-}9)$$

For the regime of the motion where $0 \leq t \leq t_o$, the above equation appears as

$$m_G\Big\{\cot\theta\left[-3\ddot{y}\cot\theta + 2.41\,a_T - 3(C_8 y + C_9)\dot{w}_y^2\right] + 5a_A\Big\}$$

$$-\frac{\mu}{C_1}\Big\{I_o\alpha + (C_5 - \mu C_4)m_I a_T$$

$$+\left[C_2 + (C_3 - \mu C_4)\tan\theta\right](F_{1y,1} + 1.41\,F_{1y,2})$$

$$+I_o\alpha - (C_6 + \mu C_4)m_I a_T$$

$$+\left[C_2 - (C_7 + \mu C_4)\tan\theta\right](F_{1y,1} + 1.41\,F_{1y,2})\Big\}$$

$$-m_I(\ddot{y} - a_A) - (F_9 + K[y - y_o]) = 0 \qquad 0 \leq t \leq t_o \quad (8\text{-}10)$$

where m_I is the mass of the inertia weight. Using $F_{1y,1}$ and $F_{1y,2}$ from Equations (6-14) and (6-15), the above equation finally appears as

$$\left[m_I + m_G \cot^2\theta \left\{ 3 - 2.41 \frac{\mu}{C_1} \left[2C_2 + \tan\theta \left(C_3 - C_7 \right. \right. \right. \right.$$

$$\left. \left. \left. \left. - 2\mu C_4 \right) \right] \right\} \right] \ddot{y} + \left[K + C_9 \omega_4^2 m_G \cot\theta \left\{ 3 - 2.41 \frac{\mu}{C_1} \left[2C_2 \right. \right. \right.$$

$$\left. \left. + \tan\theta \left(C_3 - C_7 - 2\mu C_4 \right) \right] \right\} \right] y = \left[m_I + 5 m_G \right] a_A$$

$$+ \left[m_G \cot\theta \left\{ 2.41 - \frac{2\mu}{C_1} \left[2C_2 + \tan\theta \left(C_3 - C_7 - 2\mu C_4 \right) \right] \right\} \right.$$

$$\left. - \frac{\mu}{C_1} \left(C_5 - C_6 - 2\mu C_4 \right) m_I \right] a_T - \left[C_9 \omega_4^2 m_G \cot\theta \left\{ 3 \right. \right.$$

$$\left. \left. - 2.41 \frac{\mu}{C_1} \left[2C_2 + \tan\theta \left(C_3 - C_7 - 2\mu C_4 \right) \right] \right\} + \frac{2\mu I_o \alpha}{C_1} + F_9 - K y_o \right] \quad (8\text{-}11)$$

$$0 \le t \le t_o$$

For Case II, where only the primary ball has a wedging effect on the inertia weight and $t \ge t_o$, the equilibrium requirements of the inertia weight, from Figure 12, are

$$-I_o \alpha + F_2 C_6 + F_3 C_4 + F_{1x} \left(C_5 - C_3 \right) - F_{1y} C_2$$

$$+ F_5 C_5 - F_4 C_4 = 0 \quad (8\text{-}12)$$

$$F_2 - m_I a_T - F_{1x} - F_5 = 0 \tag{8-13}$$

Motion is again assumed to be impending, so that

$$F_3 = \mu F_2 \tag{8-14}$$

$$F_4 = \mu F_5 \tag{8-15}$$

The forces F_3 and F_4 are then found to be

$$F_3 = \frac{\mu}{C_1}\left\{ I_o \alpha + (C_5 - \mu C_4) m_I a_T + \left[C_2 + (C_3 - \mu C_4)\tan\theta\right] F_{1y} \right. \tag{8-16}$$

$$F_4 = \frac{\mu}{C_1}\left\{ I_o \alpha - (C_6 + \mu C_4) m_I a_T + \left[C_2 - (C_7 + \mu C_4)\tan\theta\right] F_{1y} \right. \tag{8-17}$$

The total friction force $F_{F,TOT.}$ is

$$F_{F,TOT.} = F_3 + F_4 \tag{8-18}$$

so that

$$F_{F,TOT.} = \frac{\mu}{C_1}\left\{ 2 I_o \alpha + (C_5 - C_6 - 2\mu C_4) m_I a_T \right.$$

$$\left. + \left[2C_2 + (C_3 - C_7 - 2\mu C_4)\tan\theta\right] F_{1y} \right\} \tag{8-19}$$

For Case II operation, where only the primary ball acts on the inertia weight,

$$F_{1y,TOT.} = F_{1y,1} \tag{8-20}$$

The equilibrium requirement of the inertia weight in the y direction, from Figure 12, is

$$F_{iy,1} - F_{F,TOT} - m_I(\ddot{y} - a_A) - [F_4 + K(y - y_0)] = 0 \quad (8\text{-}21)$$

The above equation may be written as

$$m_G \cot\theta \left[-\ddot{y}\cot\theta + a_T - (C_8 y + C_9)\omega_y^2\right] + 7 m_G a_A$$

$$- \frac{\mu}{C_1}\left\{2 I_o \alpha + (C_5 - C_6 - 2\mu C_4) m_I a_T\right.$$

$$+ m_G \cot\theta \left[2C_2 + (C_3 - C_7 - 2\mu C_4)\tan\theta\right]\left[-\ddot{y}\cot\theta\right.$$

$$\left.\left. + a_T - (C_8 y + C_9)\omega_y^2\right]\right\} - m_I(\ddot{y} - a_A) - [F_4 + K(y - y_0)] = 0 \quad (8\text{-}22)$$

The term $(7 m_G a_A)$ in the above equation is added directly to account for the effect of the remaining seven balls. The terms in Equation (8-22) are combined, and the final result is

$$\left[m_I + m_G \cot^2\theta\left\{1 - \frac{\mu}{C_1}\left[2C_2 + (C_3 - C_7 - 2\mu C_4) m_I \theta\right]\right\}\right]\ddot{y}$$

$$+\left[K + C_8\omega_y^2 m_G \cot\theta\left\{1-\frac{\mu}{C_1}\left[2C_2+(C_3-C_7-2\mu C_4)\tan\theta\right]\right\}\right]y =$$

$$=\left[m_G\cot\theta\left\{1-\frac{\mu}{C_1}\left[2C_2+(C_3-C_7-2\mu C_4)\tan\theta\right]\right\}\right.$$

$$\left.-\frac{\mu}{C_1}m_I(C_5-C_6-2\mu C_4)\right]a_T+\left[\gamma m_G+m_I\right]a_N$$

$$-\left[C_9\omega_y^2 m_G\cot\theta\left\{1-\frac{\mu}{C_1}\left[2C_2+(C_3-C_7-2\mu C_4)\tan\theta\right]\right\}\right.$$

$$\left.+\frac{2\mu I_{oz}}{C_1}+F_y-K y_o\right] \qquad t\geq t_o \qquad (8\text{-}23)$$

The dimension C_2 in Figure 12 is a function of y. The effect of this is to make the equations of motion of the inertia weight, Equations (8-11) and (8-23), nonlinear. However, as is shown in Appendix B, the term C_2 exhibits a weak dependence on y. It will be assumed that the term C_2 is a constant, and the magnitude of this constant will be chosen[2] to yield conservative results for the motion

---

(2) See Appendix B for the details of this computation

of the inertia weight. If C_2 is a constant, the equations of motion of the inertia weight, Equations (8-11) and (8-23), are second order linear differential equations with constant coefficients, of the form

$$A_1 \ddot{y} + A_2 y = A_3 a_A + A_4 a_T + A_5 \alpha + A_6 \qquad (8\text{-}24)$$

where the A_j are constants.

The initial conditions are

$$t = 0 \qquad y = y_c = \text{const.} \qquad (8\text{-}25)$$

$$t = 0 \qquad \dot{y} = 0 \qquad (8\text{-}26)$$

where y_c is the initial displacement of the center of mass of the inertia weight. The above conditions are chosen to correspond to the application of the graze forcing function at $t = 0$.

9. NUMERICAL FORMS OF THE EQUATIONS OF MOTION OF THE INERTIA WEIGHT

Appendix A contains a tabulation of the numerical constants of the present problem. The particular shell considered is the 105mm Howitzer M1. Appendix B compares the forms of the equations of motion of the inertia weight for maximum and minimum values of the dimension C_2. It is seen in this appendix that the maximum percent differences between the coefficients in the equations of motion of the inertia weight, in the extreme cases, are less than 8%. It will thus be assumed, in order to obtain linear forms for the equations of motion of the inertia weight, that C_2 = constant. In addition, the constant value of C_2 will be taken to be $C_{2,MAX.}$, so that conservative(3) results will be obtained for the motion of the inertia weight. With the above assumptions, the equations of motion of the inertia weight for the two regimes $0 < t \leq t_0$ and $t_0 \leq t$ are, from Equations (8-11) and (8-23),

$$1.69 \times 10^{-4} \ddot{y} - 212 y = 3.64 \times 10^{-5} a_T + 1.37 \times 10^{-4} a_A$$

---

(3) One of the purposes of this study is to determine whether the graze module functions under the application of minimum values of the forcing functions. Equations (8-6) and (8-7) reveal that the retarding friction forces, F_2 and F_4, acting on the inertia weight will be maximum for maximum values of C_2.

$$-3.2\times10^{-6}\alpha - 141 \qquad (9\text{-}1)$$

Case I - Operation, $0 < t \leq t_2$, Balls 1 and 2 both exert wedging action on inertia weight,

$C_2 = C_{2,MAX.} = 0.476$, (Equation 8-11)

$$1.10\times10^{-4}\ddot{y} - 56.2y = 1.29\times10^{-5}a_T + 1.59\times10^{-4}a_A$$

$$-3.20\times10^{-6}\alpha - 47.7 \qquad (9\text{-}2)$$

Case II - Operation, $t_0 \leq t$, Ball 1 only exerts wedging action on inertia weight, $C_2 = C_{2,MAX.} = 0.476$, Equation (8-23)

The constraint equation which determines whether Case I or Case II operation prevails, Equation (6-27), appears as

$$\left[\ddot{y} - 2.68\times10^{6}y - 0.408a_T + 0.333a_A + 1.60\times10^{6}\right]_{t=t_0} = 0 \qquad (9\text{-}3)$$

For $0 \leq t \leq t_0$, the motion of the inertia weight will be given by Equation (9-1). For $t \geq t_0$, the motion is given by Equation (9-2). It may be observed that, for certain magnitudes of the forcing functions, there may be no positive t_0 which satisfies Equation (9-3). For this case the equation of motion of the inertia weight would be given by Equation (9-2).

10. EQUATIONS OF MOTION OF THE INERTIA WEIGHT WHEN THE GRAZE FORCING FUNCTIONS ARE APPROXIMATED BY TRIANGULAR SHAPES.

The lateral acceleration field a_T of the graze module housing will now be assumed to have the shape shown in Figure 14. By properly choosing a_0, t_1 and t_2, the best approximation to the $a_T(t)$ curve may be obtained. The three regimes of time are then

$$0 \leq t \leq t_1 \qquad a_T = \frac{a_o t}{t_1} \tag{10-1}$$

$$t_1 \leq t \leq t_2 \qquad a_T = \frac{a_o}{t_2 - t_1}(t_2 - t) \tag{10-2}$$

$$t_2 \leq t \qquad a_T = 0 \tag{10-3}$$

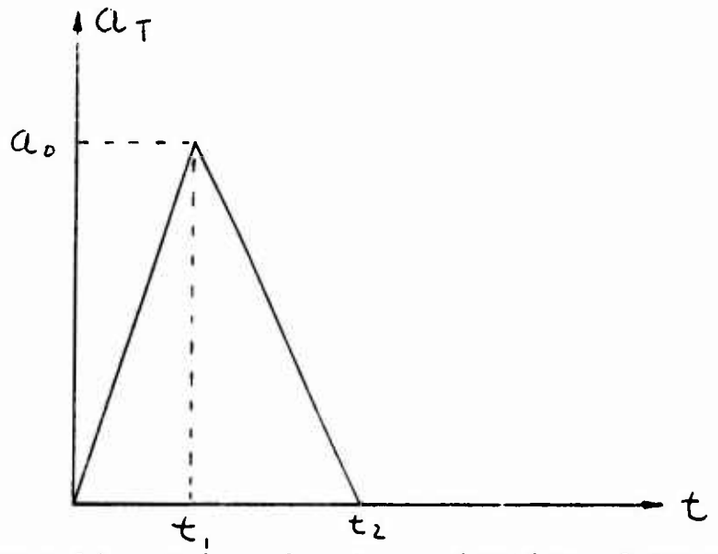

Figure 14 - Triangular Approximation of Graze Forcing Functions

where t_1 and t_2 are the times of peak and cessation, respectively, of the acceleration function.

Equation (9-1) is divided by 1.69×10^{-4}, with the result

$$\ddot{y} - 1.26 \times 10^6 y = 0.216\, a_T + 0.810\, a_A$$

$$- 0.019\, \alpha - 8.32 \times 10^5 \tag{10-4}$$

Using Equations (4-14) and (4-15), the above equation appears as

$$\ddot{y} - 1.26 \times 10^6 y = \left[0.216 + 0.810 K_1 - 0.011 K_2 \right] a_T$$

$$- 8.32 \times 10^5 \qquad (10\text{-}5)$$

K_3 is defined as

$$K_3 = \left[0.216 + 0.810 K_1 - 0.011 K_2 \right] \qquad (10\text{-}6)$$

and Equation (10-5) now appears as

$$\ddot{y} - 1.26 \times 10^6 y = K_3 a_T - 8.32 \times 10^5 \qquad (10\text{-}7)$$

Equation (10-7) will now be solved for the three regimes of operation

$0 \leq t \leq t_1$

a_T is given by Equation (10-1) as

$$a_T = \frac{a_0 t}{t_1} \qquad (10\text{-}8)$$

With

$$K_4 = \frac{K_3 a_0}{t_1} \qquad (10\text{-}9)$$

Equation (10-7) appears as

$$\ddot{y} - 1.26 \times 10^6 y = K_4 t - 8.32 \times 10^5 \qquad (10\text{-}10)$$

The complementary solution satisfies the equation

$$\ddot{y}_c - 1.26 \times 10^6 y_c = 0 \qquad (10\text{-}11)$$

or

$$y_c = A_1 \sin 1120t + A_2 \cos 1120t \qquad (10\text{-}12)$$

The particular solution y_p is assumed in the form

$$y_p = At + B \qquad (10\text{-}13)$$

Equation (10-13) is substituted into Equation (10-16), with the result

$$0 - 1.26 \times 10^6 (At + B) = K_4 t - 8.32 \times 10^5 \qquad (10\text{-}14)$$

$$-1.26 \times 10^6 A = K_4 \qquad (10\text{-}15)$$

$$-1.26 \times 10^6 B = -8.32 \times 10^5 \qquad (10\text{-}16)$$

$$A = -7.94 \times 10^{-7} K_4 \qquad (10\text{-}17)$$

$$B = 0.660 \qquad (10\text{-}18)$$

y_p is then

$$y_p = -7.94 \times 10^{-7} K_4 t + 0.660 \qquad (10\text{-}19)$$

and the general solution is

$$y = y_c + y_p \tag{10-20}$$

or

$$y = A_1 \sin 1120t + A_2 \cos 1120t$$

$$-7.94 \times 10^{-7} K_4 + 0.660 \tag{10-21}$$

The velocity $\dot{y}$ is

$$\dot{y} = 1120 A_1 \cos 1120t + 1120 A_2 \sin 1120t$$

$$-7.94 \times 10^{-7} K_4 \tag{10-22}$$

At $t = 0$, $\dot{y} = 0$, so that

$$0 = 1120 A_1 - 7.94 \times 10^{-7} K_4 \tag{10-23}$$

$$A_1 = 7.08 \times 10^{-10} K_4 \tag{10-24}$$

At $t = 0$, $y = y_c = 0.273$, so that

$$0.273 = A_2 + 0.660 \tag{10-25}$$

$$A_2 = -0.387 \tag{10-26}$$

The complete solution for the interval $0 \leq t \leq t_1$ is finally

$$y = 7.08 \times 10^{-10} K_4 \sinh 1120t - 0.387 \cosh 1120t$$

$$- 7.94 \times 10^{-7} K_4 t + 0.660 \qquad (10\text{-}27)$$

$$\dot{y} = 7.94 \times 10^{-7} K_4 \cosh 1120t - 434 \sinh 1120t$$

$$- 7.94 \times 10^{-7} K_4 \qquad (10\text{-}28)$$

In the interval $t_1 \leq t \leq t_2$ the equation of motion is

$$\ddot{y} - 1.26 \times 10^6 y = K_3 \left[\frac{a_0}{t_2 - t_1} (t_2 - t) \right] - 8.32 \times 10^5 \qquad (10\text{-}29)$$

$$= \frac{K_3 a_0 t_2}{t_2 - t_1} - \frac{K_3 a_0 t}{t_2 - t_1} - 8.32 \times 10^5 \qquad (10\text{-}30)$$

With the notations

$$K_5 = - \frac{K_3 a_0}{t_2 - t_1} \qquad (10\text{-}31)$$

$$K_6 = \frac{K_3 a_0 t_2}{t_2 - t_1} \tag{10-32}$$

Equation (10-29) appears as

$$\ddot{y} - 1.26 \times 10^6 y = K_5 t + K_6 - 8.32 \times 10^5 \tag{10-33}$$

The complementary solution is

$$y_c = A_3 \sinh 1120t + A_4 \cosh 1120t \tag{10-34}$$

The particular solution is assumed to be

$$y = Ct + D \tag{10-35}$$

Equation (10-35) is substituted into Equation (10-33), with the result

$$-1.26 \times 10^6 [Ct + D] = K_5 t + K_6 - 8.32 \times 10^5 \tag{10-36}$$

$$-1.26 \times 10^6 C = K_5 \tag{10-37}$$

$$C = -7.94 \times 10^{-7} K_5 \tag{10-38}$$

$$-1.26 \times 10^6 D = K_6 - 8.32 \times 10^5 \tag{10-39}$$

$$D = \frac{K_6 - 8.32 \times 10^5}{-1.26 \times 10^6} \tag{10-40}$$

$$D = -7.94 \times 10^{-7} K_6 + 0.660 \qquad (10\text{-}41)$$

and

$$y_p = -7.94 \times 10^{-7} K_5 t - 7.94 \times 10^{-7} K_6 + 0.660 \qquad (10\text{-}42)$$

The final solutions for y and $\dot{y}$ are then

$$y = A_3 \sinh 1120t + A_4 \cosh 1120t - 7.94 \times 10^{-7} K_5 t$$

$$- 7.94 \times 10^{-7} K_6 + 0.660 \qquad (10\text{-}43)$$

$$\dot{y} = 1120 A_3 \cosh 1120t + 1120 A_4 \sinh 1120t - 7.94 \times 10^{-7} K_5 \qquad (10\text{-}44)$$

The boundary conditions are that, at $t = t_1$, Equations (10-27) and (10-28) must be equal to Equations (10-43) and (10-44), or

$$\left[\text{Equation (10-27)} \right]_{t=t_1} = \left[\text{Equation (10-43)} \right]_{t=t_1} \qquad (10\text{-}45)$$

$$\left[\text{Equation (10-28)} \right]_{t=t_1} = \left[\text{Equation (10-44)} \right]_{t=t_1} \qquad (10\text{-}46)$$

Equations (10-45) and (10-46) are solved simultaneously for A_3 and A_4. The final result for the equation of motion in the interval $t_1 \leq t \leq t_2$ is then

$$y = \Big\{ 7.08 \times 10^{-10} K_4 \sinh 1120 t_1 - 0.387 \cosh 1120 t_1$$

$$- 7.94 \times 10^{-7} K_4 t_1 + 7.94 \times 10^{-7} K_5 t_1$$

$$+ 7.94 \times 10^{-7} K_6 \Big\} \cosh 1120 (t - t_1)$$

$$+ \frac{1}{1120} \Big\{ 7.94 \times 10^{-7} K_4 \cosh 1120 t_1 - 434 \sinh 1120 t_1$$

$$- 7.94 \times 10^{-7} K_4 + 7.94 \times 10^{-7} K_5 \Big\} \sinh 1120 (t - t_1)$$

$$- 7.94 \times 10^{-7} K_5 t - 7.94 \times 10^{-7} K_6 + 0.660 \qquad (10\text{-}47)$$

$$\dot{y} = 1120 \Big\{ 7.08 \times 10^{-10} K_4 \sinh 1120 t_1 - 0.387 \cosh 1120 t_1$$

$$-7.94 \times 10^{-7} K_4 t_1 + 7.94 \times 10^{-7} K_5 t_1$$

$$+ 7.94 \times 10^{-7} K_6 \Big\} \sinh 1120 (t - t_1)$$

$$+ \Big\{ 7.94 \times 10^{-7} K_4 \cosh 1120 t_1 - 434 \sinh 1120 t_1$$

$$-7.94 \times 10^{-7} K_4 + 7.94 \times 10^{-7} K_5 \Big\} \cosh 1120 (t - t_1)$$

$$-7.94 \times 10^{-7} K_5 \qquad \underline{t_1 \leq t \leq t_2} \qquad (10\text{-}48)$$

For $t_2 \leq t$, $a_T = 0$ and the equation of motion appears as

$$\ddot{y} - 1.26 \times 10^6 y = -8.32 \times 10^5 \qquad (10\text{-}49)$$

The solution to Equation (10-49) is

$$y = A_5 \sin 1120t + A_6 \cos 1120t + C.66 \quad (10\text{-}50)$$

and the velocity $\dot{y}$ is

$$\dot{y} = 1120 A_5 \cos 1120t + 1120 A_6 \sin 1120t \quad (10\text{-}51)$$

The above two functions must be equal to Equations (10-47) and (10-48), at $t = t_2$. This condition is expressed as

$$\left[\text{Equation (10-47)} \right]_{t=t_2} = \left[\text{Equation (10-50)} \right]_{t=t_2} \quad (10\text{-}52)$$

$$\left[\text{Equation (10-48)} \right]_{t=t_2} = \left[\text{Equation (10-51)} \right]_{t=t_2} \quad (10\text{-}53)$$

Equations (10-52) and (10-53) are solved simultaneously for A_5 and A_6. The final result for the equation of motion in the interval $t_2 \leq t$ is then

$$y = \Big\{ 7.08\times10^{-10} K_4 \sinh 1120 t_1 - 0.387 \cosh 1120 t_1$$

$$-7.94\times10^{-7} K_4 t_1 + 7.94\times10^{-7} K_5 t_1$$

$$+ 7.94\times10^{-7} K_6 \Big\} \cosh 1120 (t - t_1)$$

$$+ \frac{1}{1120} \Big\{ 7.94\times10^{-7} K_4 \cosh 1120 t_1 - 434 \sinh 1120 t_1$$

$$-7.94\times10^{-7} K_4 + 7.94\times10^{-7} K_5 \Big\} \sinh 1120 (t - t_1)$$

$$-7.94\times10^{-7} K_5 \Big[t_2 \cosh 1120 (t - t_2) + \frac{1}{1120} \sinh 1120 (t - t_2)$$

$$+ (-7.94\times10^{-7} K_6 + 0.660) \cosh 1120 (t - t_2)$$

$$- 0.660 \cosh 1120 (t - t_2) + 0.660 \qquad \underline{t_2 \leq t} \quad (10\text{-}54)$$

$$\dot{y} = 1120 \Big\{ 7.08 \times 10^{-10} K_4 \sin 1120 t_1 - 0.367 \cos 1120 t_1$$

$$- 7.94 \times 10^{-7} K_4 t_1 + 7.94 \times 10^{-7} K_5 t_1$$

$$+ 7.94 \times 10^{-7} K_6 \Big\} \sin 1120 (t - t_1)$$

$$+ \Big\{ 7.94 \times 10^{-7} K_4 \cos 1120 t_1 - 434 \sin 1120 t_1$$

$$- 7.94 \times 10^{-7} K_4 + 7.94 \times 10^{-7} K_5 \Big\} \cos 1120 (t - t_1)$$

$$- 7.94 \times 10^{-7} K_5 \Big[1120 t_2 \sin 1120 (t - t_2)$$

$$+ \cos 1120 (t - t_2) \Big]$$

$$+ (-7.94 \times 10^{-7} K_6 + 0.660) 1120 \sin 1120 (t - t_2)$$

$$- 0.660 (1120) \sin 1120 (t - t_2) \qquad \underline{t_2 \leq t} \qquad (10\text{-}55)$$

The above equations are all for the case where both the Primary Ball, 1, and the Secondary Balls, 2, exert wedging action on the inertia weight. In all of these cases, $0 < t < t_0$. The equations of motion for the case where Ball 1 alone exerts wedging action on the inertia weight, where $t_0 < t$, can be derived in a similar manner.

11. COMBINED MOTION OF INERTIA WEIGHT, DETENT BALLS AND FIRING PIN

When the inertia weight moves forward sufficiently, the two detent locking balls will be released. The orientation of the line of centers of these two balls with respect to the line of action of a_T, for the duration of the graze, is arbitrary. Figure 15 shows two extremes of this orientation. In Figure 15a both balls will have the same forces acting on them and the problem is symmetric. In Figure 15b the problem is antisymmetric, since one ball will have the a_T, effect tending to release it while the other ball will have the a_T effect opposing it.

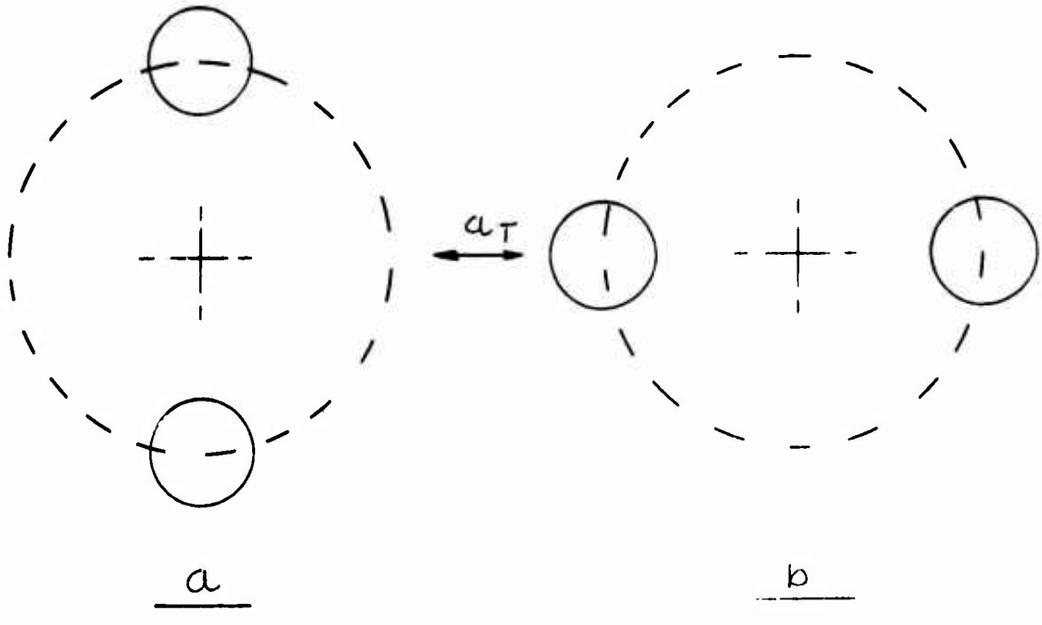

Figure 15 Detent Ball Orientation

Figure 16 shows the configuration of the firing pin, the detent ball and the inertia weight. y_1 is an axial coordinate of the firing pin, positive downwards, and y_{o1} is an arbitrary positive constant, so that the relative axial displacement of the firing pin is $y_1 - y_{o1}$. x_1 is a radial coordinate of the ball and x_{o1} is some positive constant, so that the displacement of the ball, positive outwards, is $x_1 - x_{o1}$. The displacement

of the inertia weight is $y - y_o$, as derived earlier, and the radius of the ball is designated by r. x_{o1} and y_{o1} will presently be defined.

As the inertia weight moves upward, the detent balls will move radially outward. The edge of the inertia weight will be in contact with the ball, Figure 16, for some part of the motion.

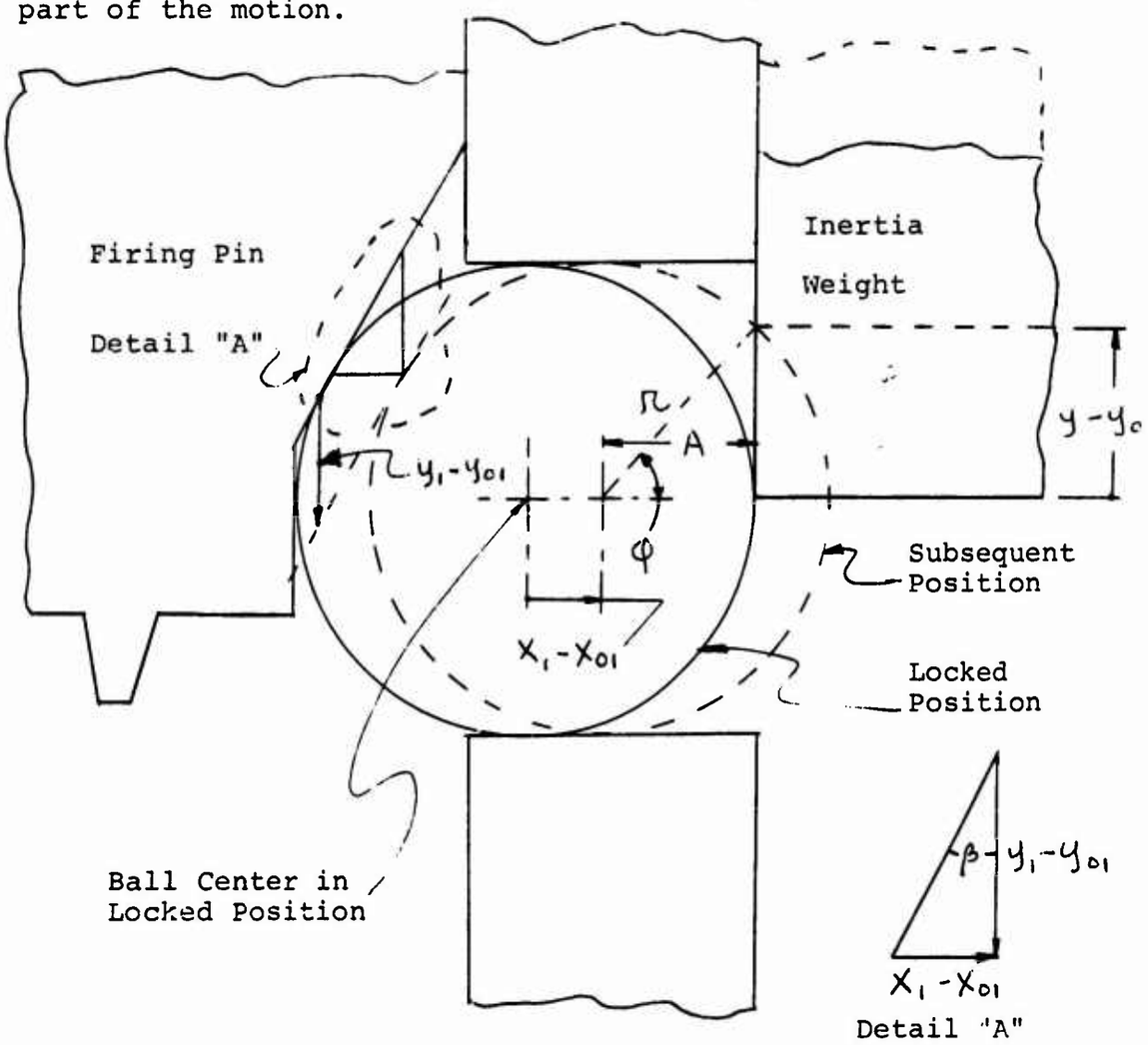

Figure 16 - Firing Pin, Detent Ball, Inertia Weight Orientation

The Kinematic relationship between the motion of the firing pin and the ball is given in Figure 16. From this figure,

$$\tan\beta = \frac{x_1 - x_{o1}}{y_1 - y_{o1}} \qquad x_1 \geq x_{o1} \qquad (11\text{-}1)$$

or

$$x_1 = 0.577\, y_1 - 0.0562 \qquad (11\text{-}1a)$$

The Dimension A in Figure 16 is given by

$$A = r - (x_1 - x_{o1}) \tag{11-2}$$

The relationship between the motion of the inertia weight and the ball, while they are both in contact, is

$$r^2 = (y - y_o)^2 + A^2 \tag{11-3}$$

or

$$r^2 = (y - y_o)^2 + \left[r - (x_1 - x_{o1}) \right]^2 \tag{11-4}$$

Equation (11-4) will be true only for the time that the ball is in contact with the inertia weight. This effect is very significant in the present derivation, and it will be subsequently discussed. From Figure 16,

$$\tan \varphi = \frac{y - y_o}{r - (x_1 - x_{o1})} \tag{11-5}$$

The relationship between the velocities $\dot{x}_1$ and $\dot{y}$ is now found by taking the first time derivative of Equation (11-4). This result is

$$0 = 2(y - y_o)\dot{y} + 2\left[r - (x_1 - x_{o1}) \right](-\dot{x}_1) \tag{11-6}$$

$$\left[\frac{y - y_o}{r - (x_1 - x_{o1})} \right] \dot{y} = \dot{x}_1 \tag{11-7}$$

With the aid of Equation (11-5), the above equation appears as

$$\dot{x}_1 = \dot{y} \tan \varphi \qquad (11\text{-}8)$$

Equation (11-8) is a kinematic relationship between the velocities of the detent ball and the inertia weight. As the ball moves radially outward, it will exert an upward component of force on the inertia weight. This force will be assumed to be small, and thus it will not influence the equation of motion of the inertia weight. Thus, the previously obtained equations of motion of the inertia weight will be valid.

As $$\varphi \rightarrow \frac{\pi}{2} \qquad (11\text{-}9)$$

$$\tan \varphi \rightarrow \infty \qquad (11\text{-}10)$$

and, following Equation (11-8),

$$\dot{x}_1 \rightarrow \infty \qquad (11\text{-}11)$$

The physical significance of Equation (11-11) is that at some angle, designated by φ_0, the ball and the inertia weight are no longer in contact. For $0 \leq \varphi \leq \varphi_0$, the motion of the detent ball bears a purely kinematic relationship to the motion of the inertia weight, in accordance with (11-8). For $\varphi_0 < \varphi$, the motion of the ball is governed by its own equation of motion. This limiting value of φ_0 will be identified in a subsequent section.

The antisymmetric case of Figure 15b will now be analyzed, with the previous assumption of quasi-static behavior. All friction forces on the detent balls will be neglected, but the friction force between the firing pin and its housing will be included. As the inertia weight moves forward several regimes of operation are possible, depending on the magnitude of the forcing functions. These regimes are identified below.

Case A - Both Detent Balls in Contact with Inertia Weight and with Firing Pin

For this case the motion relationship is purely kinematic.

The y (inertia weight) motion is related to the x_1 (detent ball) motion through Equation (11-4). The x_1 motion is related to the y_1 (firing pin) motion by Equation (11-1). From Equation (11-4),

$$y = y_o + \sqrt{R^2 - [R - (x_1 - x_{o1})]^2} \tag{11-12}$$

is the kinematic relationship between the inertia weight and the detent balls. Case A operation will exist until

$$y > y_o + \sqrt{R^2 - [R - (x_1 - x_{o1})]^2} \tag{11-13}$$

or

$$y > 0.273 + \sqrt{0.406 x_1 - x_1^2 - 3.73 \times 10^{-2}} \tag{11-14}$$

This limiting condition for Case A operation will be discussed in a subsequent section of this report.

Case B - Both Detent Balls in Contact with Firing Pin, but Not in Contact with Inertia Weight

For this case, the free body diagram will be as shown in Figure 17. The forces $P_{1,3}$ and $P_{1,4}$ are normal contact forces on Balls 3 and 4, respectively. Both balls will have equal radial displacements, since they are assumed to be in contact with the firing pin. $P_{2,3}$ and $P_{2,4}$ are reaction forces, of the detent ball guides on the detent balls, acting in the axial direction. The coordinate x_1 is measured from the center axis of the shell. x_{o1} will be taken to be the coordinate of the balls in the locked position. Thus, $x_1 - x_{o1}$ is the relative, outward, radial displacement of the balls.

Figure 18 shows the free body diagram of the firing pin, corresponding to the situation depicted in Figure 17. The coordinate y_1 is measured from the ceiling of the graze module and y_{o1} is a known constant.

If the free length of the spring is designated by a then the spring force F_s is

$$F_s = K_o (a - y_1) \tag{11-15}$$

where K_o is the spring constant. The initial spring force F_o is given by

$$F_o = K_o (a - y_{o1}) \tag{11-16}$$

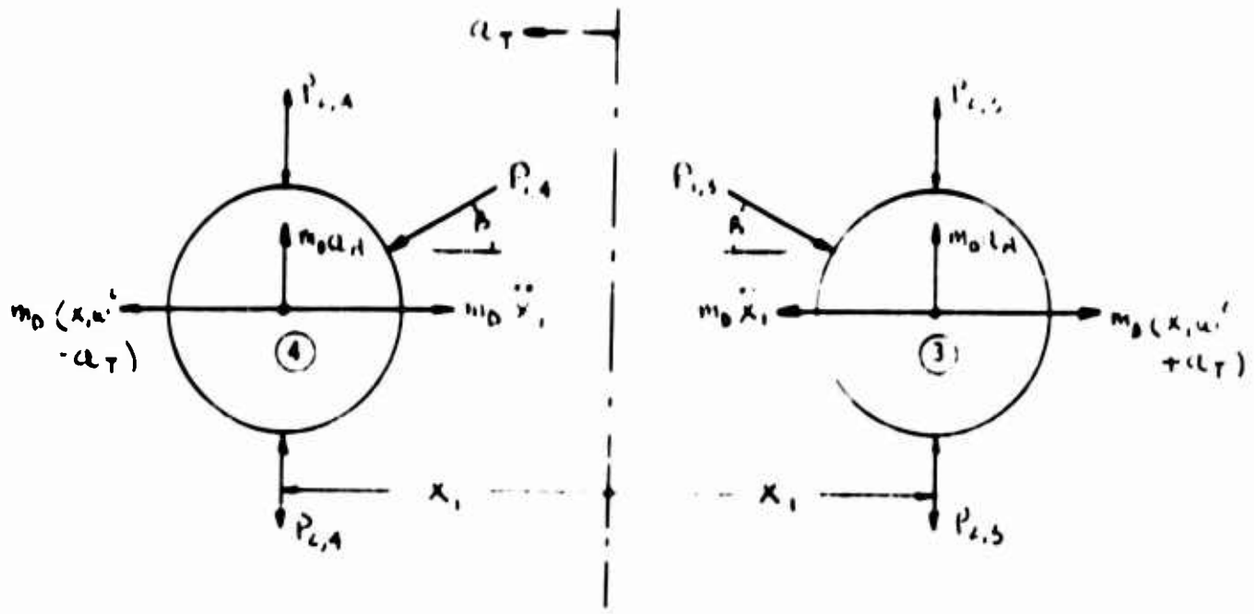

Figure 17 Free Body Diagram of Detent Balls, Case B Operation

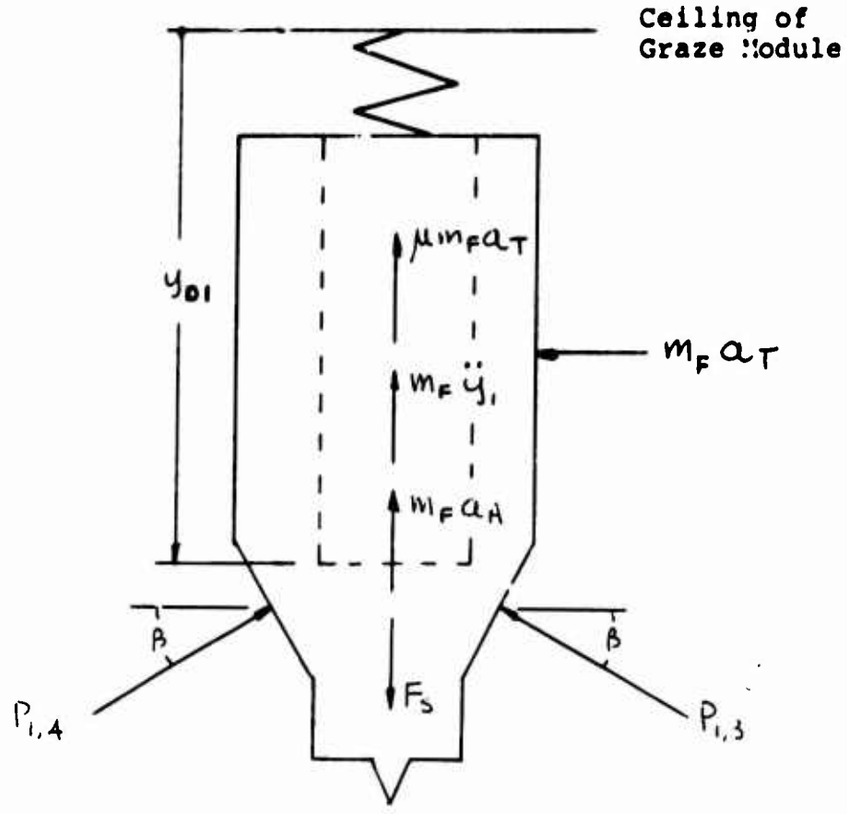

Figure 18 Free Body Diagram of Firing Pin

Equations (11-15) and (11-16) may be combined, with the result

$$F_{1,4} - F_{1,3} = K_1 (y_1 - y_{c1}) \qquad (11\text{-}17)$$

The friction force due to the normal force difference

$$(F_{1,4} - F_{1,3}) \mu_s$$

has been neglected. The equilibrium requirement of the firing pin is

$$F_0 - K_1 (y_1 - y_{c1}) - m_F g - m_F \ddot{y}_1 - c_F \dot{y}_1 - F_{1,3} \sin\beta - F_{1,4} \sin\beta = 0 \qquad (11\text{-}18)$$

and that of the detent balls is given by

$$F_{1,4} \cos\beta - m_D \ddot{x}_1 + m_D (x_{1,4} \omega_y^2 - c_T) = 0 \qquad (11\text{-}19)$$

$$F_{1,3} \cos\beta - m_D \ddot{x}_1 + m_D (x_{1,3} \omega_y^2 + c_T) = 0 \qquad (11\text{-}20)$$

where m_D and m_F are the masses of the balls and the firing pin, respectively. Equations (11-19) and (11-20) are solved for $F_{1,3}$ and $F_{1,4}$ with the result

$$F_{1,3} = \frac{1}{\cos\beta} \left[m_D \ddot{x}_1 - m_D (x_1 \omega_y^2 + c_T) \right] \qquad (11\text{-}21)$$

$$F_{1,4} = \frac{1}{\cos\beta} \left[m_D \ddot{x}_1 - m_D (x_1 \omega_y^2 - c_T) \right] \qquad (11\text{-}22)$$

From Equation (11-1),

$$\ddot{x}_1 = \ddot{y}_1 \tan\beta \qquad (11\text{-}23)$$

Equations (11-1), (11-19) and (11-21) through (11-23) are now combined and the result is

$$\left[m_F \cot\beta + 2m_b \tan\beta\right]\ddot{x}_1 - \left[2m_b \omega_y^2 \tan\beta - K_o \cot\beta\right]x_1 =$$

$$= F_o + K_o x_{o1} \cot\beta - m_F(a_A + \mu a_T) \qquad (11\text{-}24)$$

or

$$1.15 \times 10^{-5}\ddot{x}_1 + 8.60\, x_1 = 5.35$$

$$- 6.30 \times 10^{-6}(a_A + 0.1\, a_T) \qquad (11\text{-}25)$$

Equation (11-24) is the desired result for the motion of the balls when both balls are in contact with the firing pin in case B operation. It may be observed that a_T appears in Equation (11-24) only in the form of a friction force effect. After Equation (11-24) is integrated, the x_1 and y_1 motions are related by Equation (11-1). The necessary condition for case B operation is that

$$P_{1,3} > 0 \qquad (11\text{-}26)$$

$$P_{1,4} > 0 \qquad (11\text{-}27)$$

since these forces are compressive contact forces. These conditions, from Equations (11-21) and (11-22), are

$$\ddot{x}_1 - (\quad) \quad (11\text{-}28)$$

$$\ddot{x}_1 - (\quad) \quad (11\text{-}29)$$

or

$$\ddot{x}_1 - (\quad) \quad (11\text{-}30)$$

$$\ddot{x}_1 - (\quad) \quad (11\text{-}31)$$

Case C - One Ball Only in Contact with Inertia Weight

The two detent balls, from Figure 1°, experience different outward forces due to the terms $\pm a_T$. Since Ball 3 has a greater outward force on it than Ball 4, there is a possibility that it might lose contact with the firing pin before Ball 4 does. The case will now be analyzed where Ball 4 is in contact with the firing pin and Ball 3 is not.

The free body diagram for this condition is shown in Figure 19.

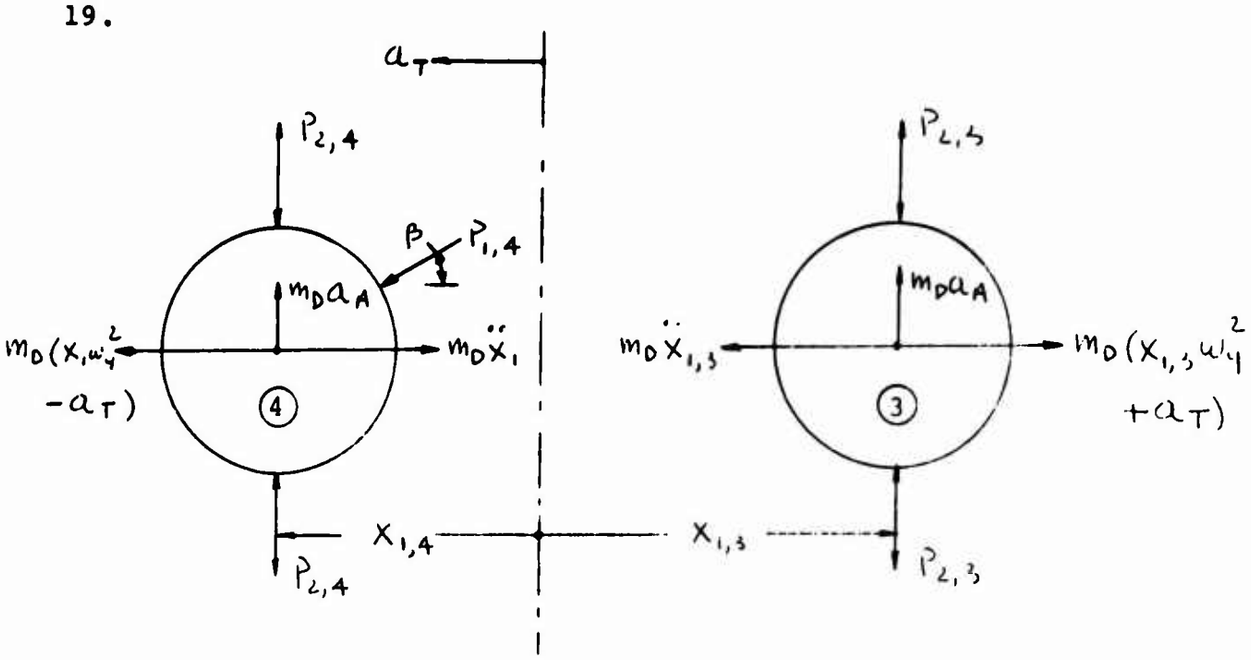

Figure 19 Free Body Diagram of Detent Balls, Case C Operation

The displacement $x_{1,4}$ of Ball 4 will be related to the displacement y_1 of the firing pin by Equation (11-1). The displacement $x_{1,3}$ of Ball 3, if $x_{1,3} > x_{1,4}$, will be independent of y_1. The free body diagram of the firing pin will be the same as that shown in Figure 19, if the force $P_{1,3}$ is removed.

The equilibrium requirement of the firing pin is

$$F_0 - K_0(y_1 - y_{01}) - m_F a_A - m_F \ddot{y}_1 - \mu m_F a_T - P_{1,4} \sin\beta = 0 \quad (11\text{-}32)$$

and that of Ball 4 is

$$P_{1,4} \cos\beta - m_D \ddot{x}_{1,4} + m_D (x_{1,4} \omega_y^2 - a_T) = 0 \quad (11\text{-}33)$$

$P_{1,4}$ is eliminated between the above two equations and, using Equation (11-1), the final result is

$$[m_F \cot\beta + m_D \tan\beta] \ddot{x}_{1,4} - [m_D \omega_y^2 \tan\beta - K_0 \cot\beta] x_{1,4} =$$

$$= F_0 + K_0 x_{01} \cot\beta - m_F (a_A + \mu a_T) - m a_T \tan\beta \quad (11\text{-}34)$$

or

$$1.12 \times 10^{-5} \ddot{x}_{1,4} + 9.6 x_{1,4} = 5.35 - 6.30 \times 10^{-6} a_A$$

$$- 9.28 \times 10^{-7} a_T \quad (11\text{-}35)$$

The equilibrium requirement for Ball 3 is

$$- m_D \ddot{x}_{1,3} + m_D (x_{1,3} \omega_y^2 + a_T) = 0 \quad (11\text{-}36)$$

and the constraint equation is

$$(x_{1,3} - x_{01}) > (y_1 - y_{01}) \tan\beta \quad (11\text{-}37)$$

The numerical form of Equation (11-36) is

$$\ddot{X}_{1,3} - [illegible] \qquad (11\text{-}38)$$

Equation (11-37) appears as

$$X_{1,3} > [illegible] \qquad (11\text{-}38a)$$

The constraint condition for Equation (11-34) is

$$P_{1,4} > 0 \qquad (11\text{-}39)$$

or, from Equation (11-29),

$$\ddot{X}_{1,4} - (X_{1,4} \omega_4^2 - a_T) > 0 \qquad (11\text{-}40)$$

or

$$\ddot{X}_{1,4} - (2.69 \times 10^6 X_{1,4} - a_T) > 0 \qquad (11\text{-}41)$$

Case D - Both Balls Not in Contact With Firing Pin or With Inertia Weight

For another regime of motion, where the firing pin exerts no force on the balls and the balls do not contact the inertia weight, the free body diagram is as shown in Figure 20.

For this case the displacements of the two balls, $X_{1,3}$ and $X_{1,4}$, are different, due to the terms $\pm a_T$. The corresponding free body diagram of the firing pin will be the same as Figure 18, with the forces $P_{1,3}$ and $P_{1,4}$ omitted.

From Figure 18,

$$F_c - K_c (y_1 - y_{c1}) - m_F a_A - m_F \ddot{y}_1 - u m_F a_T = 0 \qquad (11\text{-}42)$$

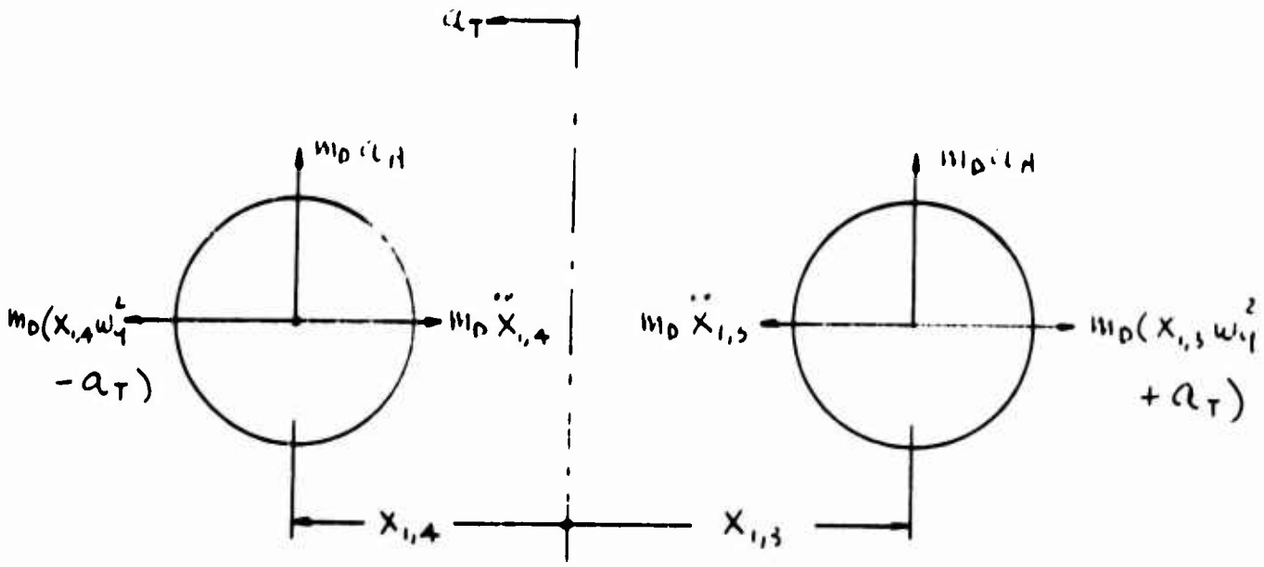

Figure 20 - Free Body Diagram of Detent Balls
Case D Operation

and, from Figure 20,

$$-m_D \ddot{X}_{1,4} + m_D(X_{1,4}\omega_y^2 - a_T) = 0 \qquad (11\text{-}43)$$

$$-m_D \ddot{X}_{1,3} + m_D(X_{1,3}\omega_y^2 + a_T) = 0 \qquad (11\text{-}44)$$

The conditions for operation in this regime are that

$$(X_{1,3} - X_{01}), (X_{1,4} - X_{01}) > (y_1 - y_{c1}) \tan\beta$$

and that Equation (11-13) is satisfied.

Equations (11-42)through (11-44) are now rearranged to appear as

$$m_F \ddot{y}_1 + K_0 y_1 = F_0 + K_0 y_{01} - m_F (a_A + \mu_1 a_T) \quad (11\text{-}45)$$

$$\ddot{x}_{1,4} - \omega_y^2 x_{1,4} = -a_T \quad (11\text{-}46)$$

$$\ddot{x}_{1,3} - \omega_y^2 x_{1,3} = a_T \quad (11\text{-}47)$$

or

$$6.30 \times 10^{-6} \ddot{y}_1 + 6.00 y_1 = 5.94 - 6.30 \times 10^{-6} (a_A + 0.1\ a_T) \quad (11\text{-}48)$$

$$\ddot{x}_{1,4} - 2.69 \times 10^6 x_{1,4} = -a_T \quad (11\text{-}49)$$

$$\ddot{x}_{1,3} - 2.69 \times 10^6 x_{1,3} = a_T \quad (11\text{-}50)$$

The coordinate y is a measure of the axial displacement of the inertia weight, while the coordinate y_1 measures the axial displacement of the firing pin. For computer solutions of the present problem, it may be more efficient to express all results in terms of y . The transformation equations which relate y and y_1 , and their derivatives, are

$$y + y_1 = C_{11} = 0.549 \quad (11\text{-}51)$$

$$\dot{y} = -\dot{y}_1 \quad (11\text{-}52)$$

$$\ddot{y} = -\ddot{y}_1 \quad (11\text{-}53)$$

12. LIMITING CONDITIONS FOR INERTIA WEIGHT TO BE IN CONTACT WITH DETENT BALLS

The combined motion of the inertia weight, detent balls and firing pin is an effect which exhibits bilinear behavior. In addition, for a small part of the motion of the detent balls the motion may be nonlinear, and this situation shall be discussed in the following paragraph. Numerical values of the forcing functions are required before a definite identification can be made of the various regimes of combined motion of the detent balls and firing pin.

Figure 21 shows the detent ball at the last point at which it is tangent to the inclined surface of the firing pin. As the pin moves down further, and if it still contacts the ball, the magnitude and direction of the contact force will continually be changing. This will be a regime of nonlinear motion because of the changing direction of the force.

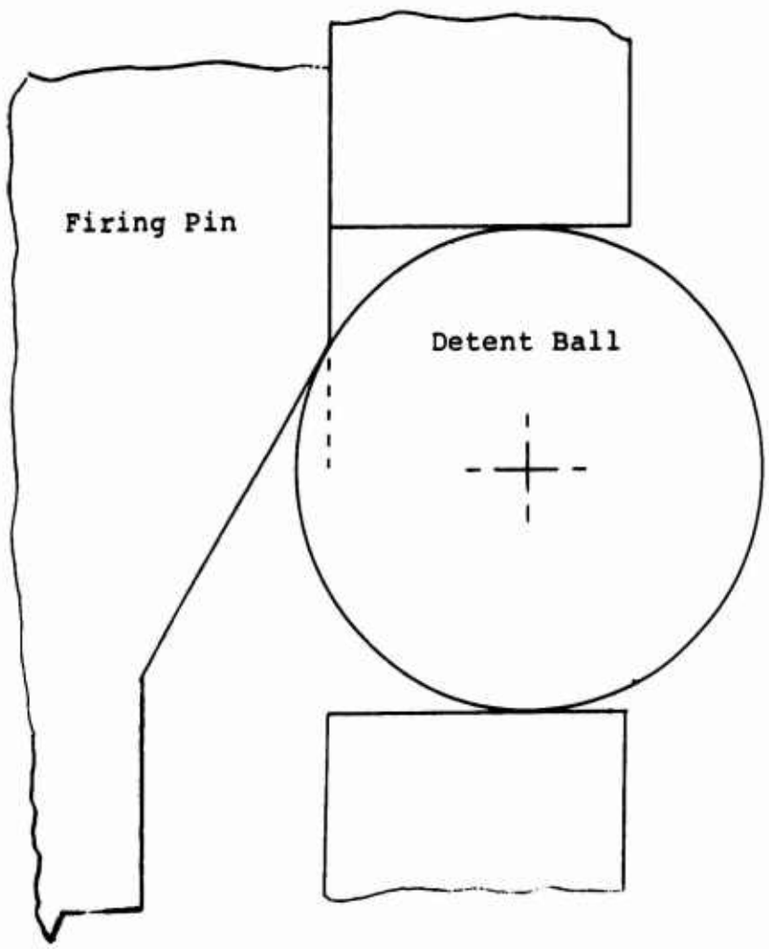

Figure 21 - Kinematic Relationship of Firing Pin and Detent Ball

Since this motion is a small part of the total motion, it will be treated as a linear motion. That is, when the pin goes down past the position shown in Figure 21, it will be assumed that there is no further contact between the pin and the detent ball. From Figure 22, when a detent ball has moved through a radial distance C_{12}, it will be assumed to no longer be in contact with the firing pin.

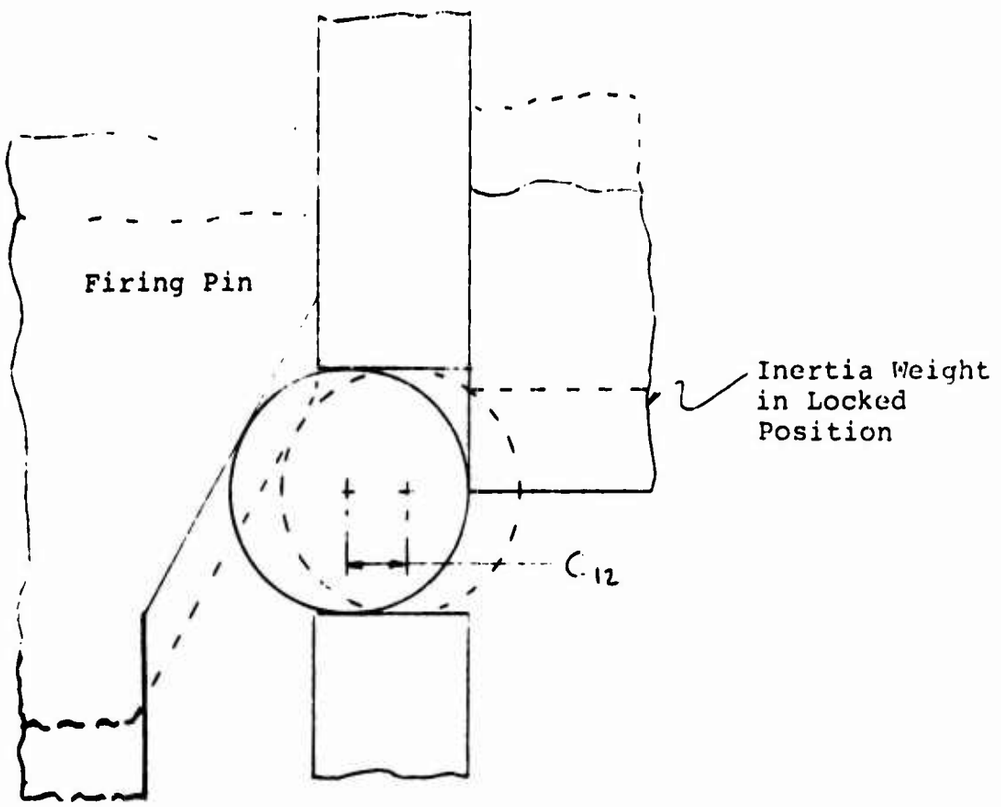

Figure 22 - Limiting Position of Firing Pin and Detent Ball

In the initial configuration, at time $t = 0^-$, the inertia weight is down, Figure 1, and the detent balls are in the locked position. At $t=0$ the graze forcing functions are applied and at some later time, for sufficiently large values of the forcing functions, the inertia weight begins to rise. In this initial stage of the motion balls (1) and (2) are in contact with the inertia weight, in Case A Operation. A method of superposition will now be employed to determine the time and position at which this contact is lost.

For Case A operation, the displacements and velocities of the balls and the inertia weight are related by Equations (11-4) and (11-8). Also, at the outset of motion both detent balls are in positive contact with the firing pin.

The inertia weight will now be imagined to be removed and the equation of motion, Equation (11-24), for the situation of Figure 17, will be solved. This solution will be called $X_{I,a}(t)$. The kinematic relationships between the inertia weight and the balls are repeated below

$$r^2 = (y - y_0)^2 + \left[r - (x_1 - x_{01}) \right]^2 \tag{12-1}$$

$$\dot{x}_1 = \dot{y} \tan\varphi \tag{12-2}$$

The function y is the motion of the inertia weight and at this stage of the analysis is a known function of time. The term x_1 in the above two equations will be designated by $x_{1,b}(t)$ and these two equations are rewritten as

$$x_{1,b} = x_{01} + r - \sqrt{r^2 - (y - y_0)^2} \tag{12-3}$$

$$\dot{x}_{1,b} = \dot{y} \tan\varphi \tag{12-4}$$

The inertia weight is now placed back in the problem. Contact between the balls and the inertia weight will then be maintained so long as

$$x_{1,a} \geq x_{1,b} \tag{12-5}$$

This expression implies that the X_1 motion of the balls for this hypothetical case is "ahead" of the X_1 motion of the inertia weight. The limiting condition when contact is lost occurs when

$$\left[X_{1,a} = X_{1,b} \right]_{t=t_4} \tag{12-6}$$

Both $X_{1,a}$ and $X_{1,b}$ are known functions of time, after the forcing functions have been described. The time t_4 which satisfies Equation (12-6) may now be found, and this time t_4 is the time at which the inertia weight loses contact with the detent balls, at the end of Case A operation.

The relationship

$$\left[\dot{X}_{1,a} = \dot{X}_{1,b} \right]_{t=t_4} \tag{12-7}$$

may be used to find φ_c, the limiting angle which was defined in the section following Equation (11-11).

13. SUMMARY OF EVENTS DURING THE TOTAL FUNCTIONING TIME FROM GRAZE TO FIRING

In order for the graze module to be effective in performing its design function it must open sufficiently to release the detent balls which, in turn, release the firing pin. The test of whether the inertia weight moves forward with respect to the shell is as follows.

a. The solution for y, from Equation (8-11) and (9-1), or from Equation (8-23) and (9-2), must be positive. A positive value of y would indicate that the inertia weight moves forward with respect to the graze module housing.
b. The velocity, $\dot{y}$, of the inertia weight must be positive. In view of the definition of the orientation of the secondary x, y, z coordinates, a negative value of $\dot{y}$ would be incompatible with the physical constraints of the problem.

The graze forcing functions are assumed to be applied at time $t = 0^+$. At this outset of motion of the inertia weight two regimes of motion are possible, if the magnitude of the graze force is sufficiently large. In one of these regimes, both the primary and the secondary balls will exert wedging action on the inertia weight, and the equation of motion of this weight is expressed, in its most fundamental form, by Equation (8-11) or (9-1). This will be Case I Operation, as previously defined. For this regime of motion the inequality, Equation (6-33), must be satisfied. If Equation (6-33) is not satisfied, then only the primary ball will exert wedging action on the inertia weight. For this case, previously defined as Case II Operation, the equation of motion of the inertia weight is given by Equation (8-23) or (9-2).

If the magnitudes of the graze forcing functions are not sufficiently large, the inertia weight will not open. In the following discussion it will be assumed that the forcing functions which are applied at $t = 0^+$ result in

$$y > 0 \qquad t > 0 \tag{13-1}$$

$$\dot{y} > 0 \qquad t > 0 \tag{13-2}$$

This assumption may be tested when the numerical results are obtained.

The several possible regimes of motion which follow the opening of the inertia weight will now be considered. It must be emphasized that a positive identification of a particular regime of operation will be possible only after the numerical values of the forcing functions have been specified. Consideration will now be given to the combined motion of the inertia weight, detent balls and firing pin. There are several possible sequences of events which may occur after the application of the forcing functions. Two typical sequences will be presented below.

In the first of these sequences, designated as Circuit 1, the sequence will be

Case A ⟶ Case B ⟶ Case D

where the cases are defined in section 11.

When both detent balls have moved through a distance C_{12}, Figure 22, the firing pin is free to close. In the second sequence, designated by Circuit 2, Case A Operation will be assumed to exist until both detent balls have moved radially through a distance C_{12}. The equation of motion of the firing pin will then be as outlined in Case D. Other sequences may exist, depending on the numerical values. The computations below, however, outline the typical details of going through a particular circuit.

Circuit 1

At the outset of motion, at $t = 0^+$, the inertia weight is in the downward position displayed in Figure 1. In this position, which is Case A Operation, both detent balls are in positive contact with the inertia weight. If the forcing functions are of sufficient magnitude to cause the inertia weight to commence its opening process, then a limiting condition occurs when the inertia weight loses contact with the two detent balls. This condition will occur at a time designated by t_4 where t_4 is the time which satisfies Equation (12-6). The time t_4 is now compared with t_o where t_o is given by Equation (6-26). If $t_4 < t_o$, then the solution of Equation (9-1) is evaluated at $t = t_4$. This value will be designated by y_A, where y_A is a constant. It will represent the upward travel of the inertia weight which corresponds to the time t_4.

If $t_4 > t_o$ the problem is inherently more difficult. A test is first made to ascertain whether t_o is positive. If t_o is not positive, then the two secondary balls (2) do not exert any wedging effect on the inertia weight. For this case the solution of Equation (9-2) is evaluated at $t = t_4$.

This value will be designated by y_B , where y_B is a constant, and it will represent the upward travel of the inertia weight which corresponds to t_4 .

If $t_4 > t_o$, and $t_o > 0$, then for part of the travel of the inertia weight all three balls will exert wedging action, and for another part of the travel only the primary ball will exert this action. The solution for $t < t_o$ will be designated by y_C , and it may be found from Equation (9-1). The solution for $t_o < t < t_4$ will be designated by y_D . The initial conditions for this problem are then

$$t = 0 \qquad y_C = y_c \tag{13-4}$$

$$\dot{y}_C = 0 \tag{13-5}$$

$$t = t_o \qquad y_C = y_D \tag{13-6}$$

$$\dot{y}_C = \dot{y}_D \tag{13-7}$$

The total displacement of the inertia weight at time t_4 , designated by y_E , is then

$$y_E = y_D \Big|_{t = t_4} \tag{13-8}$$

The initial conditions for the solutions which result in y_A and y_B are

$$t = 0 \qquad y = y_c \tag{13-9}$$

$$t = 0 \qquad \dot{y} = 0 \tag{13-10}$$

At this stage of the analysis there are three possible displacements of the inertia weight which may exist, and these are y_A, y_B or y_E. The several values of the displacement of the inertia weight, at the point where it loses contact with the detent balls, are summarized below.

$$t_o > 0 \qquad t_4 < t_o \qquad y\Big|_{t=t_4} = y_A \tag{13-11}$$

$$t_o < 0 \qquad t_4 > t_o \qquad y\Big|_{t=t_4} = y_B \tag{13-12}$$

$$t_o > 0 \qquad t_4 > t_o \qquad t < t_o \qquad y = y_c \tag{13-13}$$

$$t_o > 0 \qquad t_4 > t_o \qquad t_o < t < t_4 \qquad y = y_D \tag{13-14}$$

$$t_o > 0 \qquad t_4 > t_o \qquad y\Big|_{t=t_4} = y_D\Big|_{t=t_4} = y_E \tag{13-15}$$

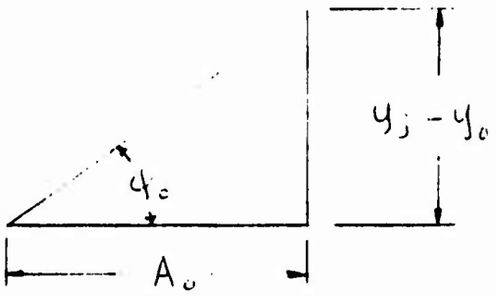

Figure - 23 Kinematic Relationships

Figure 23 shows a detail from Figure 16. The subscribt j may be A, B or E. φ_o is the limiting angle at which the inertia weight looses contact with the detent ball, defined by Equation (12-7), and A_o corresponds to φ_o . From Equation (11-2)

$$A = r - (x_1 - x_{01}) \tag{13-16}$$

From the figure

$$A_o = (y_j - y_c) \cot \varphi_o \tag{13-17}$$

$x_{1,j}$ will be the radial displacement of the detent balls, at the position $\varphi = \varphi_o$, which corresponds to y_j , where j = A, B or E. Equation (13-16) is substituted into Equation (13-17), with the result

$$(y_j - y_c) \cot \varphi_o = r - (x_{1,j} - x_{01}) \tag{13-18}$$

or

$$x_{1,j} = x_{01} + r - (y_j - y_c) \cot \varphi_o \tag{13-19}$$

Equation (13-19) gives the radial location of the detent balls at the time t_4 when the inertia weight loses contact with these balls. The corresponding velocities of the detent balls may be found with the aid of Equation (11-8) which appears as

$$\left[\dot{x}_1 = \dot{y} \tan \varphi\right]_{t=t_4} \tag{13-20}$$

The functional forms of $\dot{y}$ have already been obtained for the several regimes of time which are defined by Equations (13-11) through (13-15), and the initial conditions. The values of $\dot{y}_j$, where $j = A, B$ or E, may then be obtained for $t = t_4$. The detent ball velocity $\dot{x}_{1,j}$ is then related to the inertia weight velocity $\dot{y}_j$, following equation (13-20), by

$$\dot{x}_{1,j} = \dot{y}_j \tan \varphi_o \tag{13-21}$$

where φ_o is as previously defined and $j = A, B$ or E.

In Circuit 1 Operation, Case B Operation is assumed to follow Case A Operation. This implies that, from Figure 22,

$$x_{1,j} - x_{01} < c_{12} = 0.039 \tag{13-22}$$

$$x_{1,j} < 0.179 \tag{13-23}$$

The two detent balls are in contact with the firing pin, but no longer in contact with the inertia weight. The motion of the detent balls is given by Equation (11-24). This equation is integrated, and the solution is designated by x_1^B, where the superscript B signifies Case B Operation.

The initial conditions are

$$t = t_4 \qquad x_1^B = x_{1,j} \qquad j = A, B \text{ or } E \tag{13-24}$$

$$t = t_4 \qquad \dot{x}_1^B = \dot{x}_{1,j} \qquad j = A, B \text{ or } E \tag{13-25}$$

When

$$x_1^B - x_{01} = c_{12} \tag{13-26}$$

or

$$x_1^B = c_{12} + x_{01} \tag{13-27}$$

the detent balls lose contact with the firing pin and Case B Operation ceases. The corresponding time is t_5. For $t > t_5$, Case D Operation prevails and the equation of motion of the firing pin is given by Equation (11-45). Following Equation (11-1),

$$(y_1 - y_{01}) \tan\beta = x_1 - x_{01} \tag{13-28}$$

For the conditions of Equation (13-26), Equation (13-28) appears as

$$(y_1 - y_{01}) = c_{12} \cot\beta \tag{13-29}$$

and, from Equation (11-1),

$$\dot{y}_1 = \dot{x}_1 \cot\beta \tag{13-30}$$

Equation (11-45) is now integrated, and the solution is designated y_1^D. The initial conditions are

$$t = t_5 \qquad y_1^D - y_{01} = c_{12} \cot\beta \tag{13-31}$$

$$t = t_5 \qquad \dot{y}_1^D = \dot{x}_1^B \Big|_{t=t_5} \cot\beta \tag{13-32}$$

If the maximum travel of the firing pin is $y_{1,MAX} - y_{C1}$ and the corresponding time at the end of this travel is t_6 , then

$$\left(y_1^D - y_{C1} \right) \Big|_{t=t_6} = y_{1,MAX.} - y_{C1} \qquad (13\text{-}33)$$

Equation (13-33)may be used to find t_6 . The velocity of the firing pin on striking the detonator is

$$\dot{y}_1^D \Big|_{t=t_6}$$

and the kinetic energy of the firing pin on impact is

$$KE = \frac{1}{2} m_F \left[\dot{y}_1^D \Big|_{t=t_6} \right]^2 \qquad (13\text{-}34)$$

Circuit 2

In Circuit 2 Operation, the inertia weight is assumed to remain in contact with both detent balls until these balls have moved through a radial distance C_{12} . The corresponding time will be designated by t_7 . As in Circuit 1 Operation, a preliminary test is whether $t_7 > t_6$ or $t_7 < t_6$, and this analysis would follow the steps outlined earlier. The condition when the detent balls lose contact with the firing pin is

$$t = t_7 \qquad x_1 - x_{01} = C_{12} \qquad (13\text{-}35)$$

The displacement of the inertia weight at $t = t_7$ is given by $y|_{t=t_7}$. When Equation (13-35) is substituted into Equation (11-4), the result is

$$\left(y\Big|_{t=t_7} - y_0 \right) = + \sqrt{R^2 - (R - C_{12})^2} \qquad (13\text{-}36)$$

Time t_7 may now be found from Equation (13-36). The corresponding velocity of the detent balls is, from Equations (11-5) and (11-8),

$$\dot{x}_1\Big|_{t=t_7} = \left[\frac{y|_{t=t_7} - y_0}{R - C_{12}} \right] \dot{y}\Big|_{t=t_7} \qquad (13\text{-}37)$$

The displacement and velocity of the firing pin at $t = t_7$, following the form of Equation (13-29), are

$$t = t_7 \qquad \left(y\Big|_{t=t_7} - y_{01} \right) = C_{12} \cot\beta \qquad (13\text{-}38)$$

$$t = t_7 \qquad \dot{y}_1\Big|_{t=t_7} = \dot{x}_1\Big|_{t=t_7} \cot\beta \qquad (13\text{-}39)$$

The motion of the firing pin for $t > t_7$ is given by Equation (11-45). The integral of this equation is designated by y_1^E. The initial conditions are, using Equations (13-36) through (13-39).

$$t = t_7 \qquad \left(y_1^E - y_{01} \right) = C_{12} \cot\beta \qquad (13\text{-}40)$$

$$\dot{y}_1^E = \cot\beta \left[\frac{\sqrt{r^2 - (r - c_{12})^2}}{r - c_{12}} \right] \ddot{y} \Big|_{t = t_7} \qquad (13\text{-}41)$$

When the final form of y_1^E is obtained the solution proceeds as before, starting with Equation (13-33).

All of the numerical values of the constants in this section are contained in Appendix A.

14. DISCUSSION OF ASSUMPTIONS

The purpose of the present report is to investigate the effectiveness of the graze module of the Hi-Performance point detonating fuze. The assumptions which are the basis for this study will now be commented on. It should be emphasized that, since no numerical results are obtained in this study, certain conclusions must, of necessity, be general.

Assumption a, which states that the direction of a_T is constant with respect to the position of a particular graze ball, reduces the situation to a static analysis of a dynamical problem. If t_B is the time for any graze ball to occupy a successive position, then

$$t_B = \pi / 4\omega_y \qquad (14\text{-}1)$$

where ω_y is the assumed constant spin velocity of the shell. If the total time from the initiation of graze to the firing event is much less than t_B, then assumption a can be justified. If this situation does not prevail, the analysis would have to be modified to show the time varying effect, due to shell rotation, of a_T on the graze balls. In the present analysis, a_T is assumed to have a constant direction with respect to the graze balls, as shown in Figure 3. In the more refined analysis, the effect of a_T along a radial axis through the graze balls would be of the form

$$a_T A \sin(\omega_y t + \theta_0) \qquad (14\text{-}2)$$

where α_0 is a conveniently chosen phase angle. The above conclusion also applies to assumption g, (page 11), which assumed that the direction of a_T is constant with respect to the direction of the two detent balls.

Assumption b states that friction forces exist only between the inertia weight and the center post, and between the firing pin and the center post. The friction forces which have been neglected are those between the graze balls and their mating surfaces. As the graze balls move radially inward, they will possess a combined rotating and translating motion. The normal contact forces on the graze and detent balls were defined earlier. It is thus possible to compute the tangential friction forces acting on the graze balls, after the motion has been established. A similiar line of reasoning applies to the tangential friction forces acting on the detent balls. When these friction forces are obtained, they may be compared to the other forces acting on the balls, and the validity of the assumption may be tested.

Assumption c states that the coefficient of friction between all sliding parts is constant. This standard assumption is usually true for the case of low contact pressures between the surfaces in contact. In the present problem, the impact nature of the graze forcing functions may cause considerable contact pressures between the graze balls and their contacting surfaces. As a result, the coefficients of static and kinetic friction may be considerably higher than the present estimates. In these cases, the coefficients are found to be dependent on the relative velocity, at a given pressure value, of the mating surfaces. The maximum value of the constant coefficient of friction in the present problem is assumed to be 0.1. If solutions are obtained for $\mu = 0.1$, and $\mu = 0$, the range of the effect of friction forces on the problem can be determined. In a more refined analysis of the problem, the variation of the coefficient of friction should be considered.

Assumptions d and e exclude all gyrodynamic effects of the moving shell. Assumption d describes the shell as possessing only constant spin velocity. When the shell grazes the terrain, there will be a decrease in this spin velocity of unknown magnitude. The centrifugal forces on the graze balls, caused by the spin velocity, tend to retard the functioning of the graze module assembly. By assuming the spin velocity to be constant, a test is made of whether the graze module will function under the most adverse condition. If the numerical results indicate a borderline situation of operation, then a more refined analysis could include an assumed functional form for the decrease with respect to time of the spin velocity.

For this case the tangential (i.e. in a direction normal to the radial grooves) inertia forces on the graze balls would have to be included. The remaining two rotation components in the present problem, ω_x and ω_z, of the shell absolute rotational velocity are assumed to be much smaller than ω_y, and are thus neglected.

Assumption e states that the shell moves in a plane which is normal to the graze terrain, and remains at a constant angle with respect to this terrain. This assumption implies that the shell impacts the terrain with zero angle of attack, and that there is no spin decay. As the shell grazes the terrain, it is acted upon by some net external moment. Since there will be a change in all three components of the shell absolute rotational velocity, the shell must change its direction in such a way as to continually satisfy the moment-moment of momentum equation. The net result of this will be that the shell, at some time, will move out of its original direction. The magnitudes and durations of the graze forcing functions cover a wide range of values. In addition, these values are not known with great accuracy. It is the anticipation of the present design of the graze module that the total time from the initiation of graze to the firing event is small compared to other times in the problem. It thus appears that the above assumption, which states that the shell direction is constant with respect to the graze terrain, is reasonable. This assumption can more accurately be tested when the numerical results are obtained.

Assumption j states that the graze balls translate only in a plane through the center axis of the graze module. As the graze balls move radially in their grooves, there will be coriolis inertia forces which tend to displace the balls in a direction normal to these grooves. In addition, there will be components of the inertia force which tend to displace certain of the balls laterally. This latter effect is shown in Figure 24.

The two balls in the upper part of the figure, for the position shown, will have acting on them inertia forces, in a direction normal to the grooves, of magnitude $m_6 a_T \sin 45^\circ$. It is assumed in the present study that the effects of these forces, and of the coriolis inertia forces, are small compared to the other forces acting on the balls. These forces could be included in a more refined analysis of the graze module. The tangential inertia forces on the graze balls, which are absent because of assumption d, are also neglected.

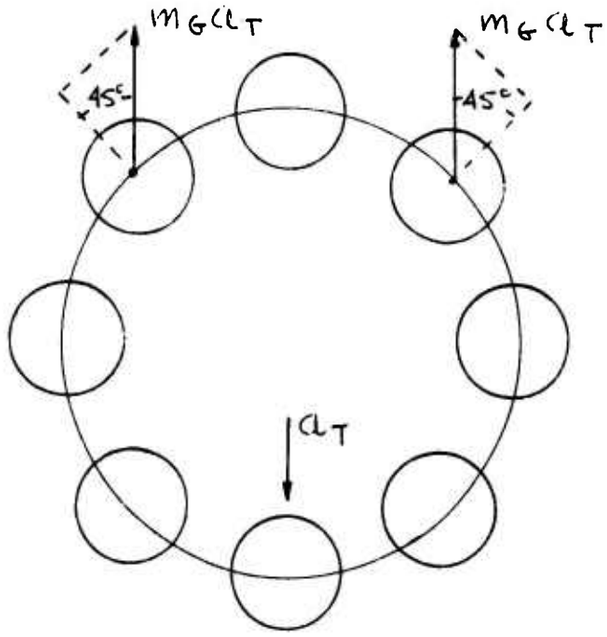

Fig. 24 - Tangential Effect, due to a_T, on Graze Balls

Assumption h assumes that the dimension C_2 is constant, so that the equations of motion will have linear forms. Appendix B contains the details of the computation of the range of values of C_2 . A constant value of this term is chosen which will yield conservative results for the motion of the inertia weight. It is the feeling of the present author that the error introduced by assuming C_2 to be constant is less than the uncertainty in the magnitudes of the actual graze forcing functions.

Assumption i assumes, merely for convenience, that the graze force acts at the tip of the ogive shell nose.

Assumption j states that the mass moment of inertia of the firing pin, about an axis through its center of mass and normal to the longitudinal axis of the shell, may be neglected. This assumption is made since the firing pin is a slender element which, for a considerable part of its length, has the shape of a thin walled shell. It should be observed that this assumption was not made for the inertia weight, since this element has a shape which resembles a thick disc.

Assumption K states that the firing pin moves only forward with respect to the graze module housing. When the detent balls move outward sufficiently, the firing pin is free to

move forward under the influence of the firing pin spring. The axial friction force on the firing pin will always act to oppose the motion, so that this friction force on the firing pin will have a sense which is towards the nose of the shell. This effect is reflected in the sign of the terms $\mu m_F a_T$ in Equations (11-18), (11-32) and (11-42. The criteria of whether the firing pin does indeed move forward are

$$y_1 - y_{01} > 0 \qquad (14\text{-}3)$$

and

$$\dot{y}_1 > 0 \qquad (14\text{-}4)$$

If this situation does not prevail, then the signs of the terms $\mu m_F a_T$ in the above referenced equations are changed for the regime of motion where the firing pin moves towards the nose of the shell. The initial conditions of the firing pin would, of course, have to be modified accordingly.

Assumption l states that the firing pin spring is a massless element with a constant spring rate. This appears to be a valid assumption for a first approximation solution of the present problem. This spring tends to be compressed by the inertia forces induced by the direct effect of a_A on the mass particles of the spring. In addition, the firing pin spring has a mass which is not negligible compared with the mass of the firing pin. It is possible, then, that the spring force which is actually available to accelerate the firing pin may be much less than the design value which is used in this study.

Assumption m approximates the true graze forcing functions by a triangular shape. The general shape of the actual forcing function is shown in Figure 25. An improvement in the representation of the forcing functions may be obtained by a combination of the functions

$$e^{ut} \text{ and } e^{vt}$$

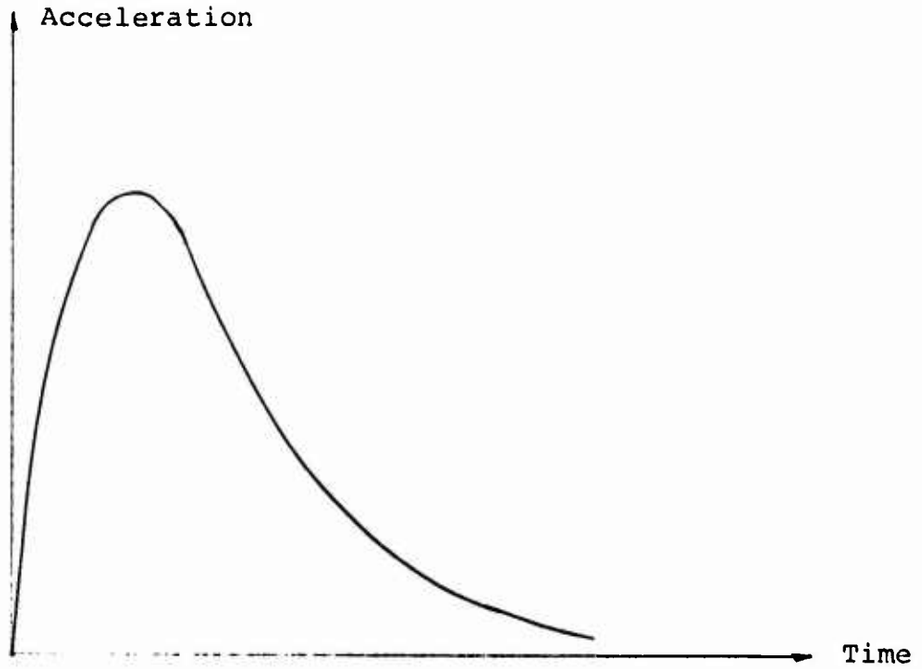

Fig. 25 - Typical Acceleration - Time Function at Impact

This new function for the acceleration a_T would be of the form

$$a_T = A\left(e^{ut} - e^{vt}\right) \qquad (14\text{-}5)$$

where A, u and v are constants to be chosen, and

$$u, v < 0 \quad \text{and} \quad u > v$$

These constants may then be selected so that the best approximation to the actual curve is obtained.

15. CONCLUSIONS AND RECOMMENDATIONS

An analysis has been made of the major elements of the graze module of the Hi-Performance point detonating fuze, subject to the assumptions which are described in this report. The analysis shows a favorable form of solution for the equation of motion of the inertia weight, and this is an important factor in the sequential operation of the graze module. The analysis identifies two cases for the combined motion of the inertia weight and the graze balls, and four cases for the sequential motion of the inertia weight - detent balls - firing pin. Any combination of these latter cases may occur, depending on the values of the graze forcing functions. A numerical form of each equation was obtained, based on present design parameters for the 105 mm Howitzer, M1. The forcing functions in one section of the report were also approximated by triangular shapes. No numerical values are obtained in this report. These values must be known before definite judgements may be made of the assumptions.

The following recommendations are offered for future study.

a. the dependence of the acceleration a_T on the shell rotation
b. the effect of spin decay on the equations of motion
c. the effect of the tangential inertia forces (i.e. in a direction normal to the radial grooves) on the graze balls
d. the dynamic effects of the firing pin spring, and of the inertia weight creep springs
e. the inclusion of a more accurate representation of the graze forcing functions
f. the inclusion in the impact configuration of the initial yaw angle of the shell. This analysis, together with the inclusion of spin decay, would provide more detailed results for the gyrodynamic motion of the shell during impact, and its instability behavior thereafter.
g. the effect of a variable coefficient of friction on the motion of the graze module components.

APPENDIX A - EVALUATION OF THE CONSTANTS OF THE PROBLEM

a. Location of The Centroid of The Inertia Weight

Figure A-1 shows the nominal dimensions of the inertia weight. In the calculation of the location of the centroid and the moment of inertia about the centroid, the following portions of the inertia weight will be neglected

1. The groove, as shown in Figure A-1
2. The 0.0625 locating hole
3. The 0.219 hole

As a preliminary calculation, the centroid of a frustrum of a right circular cone will be obtained. Figure A-2 shows the solid, and it is also piece "A" in Figure A-1.

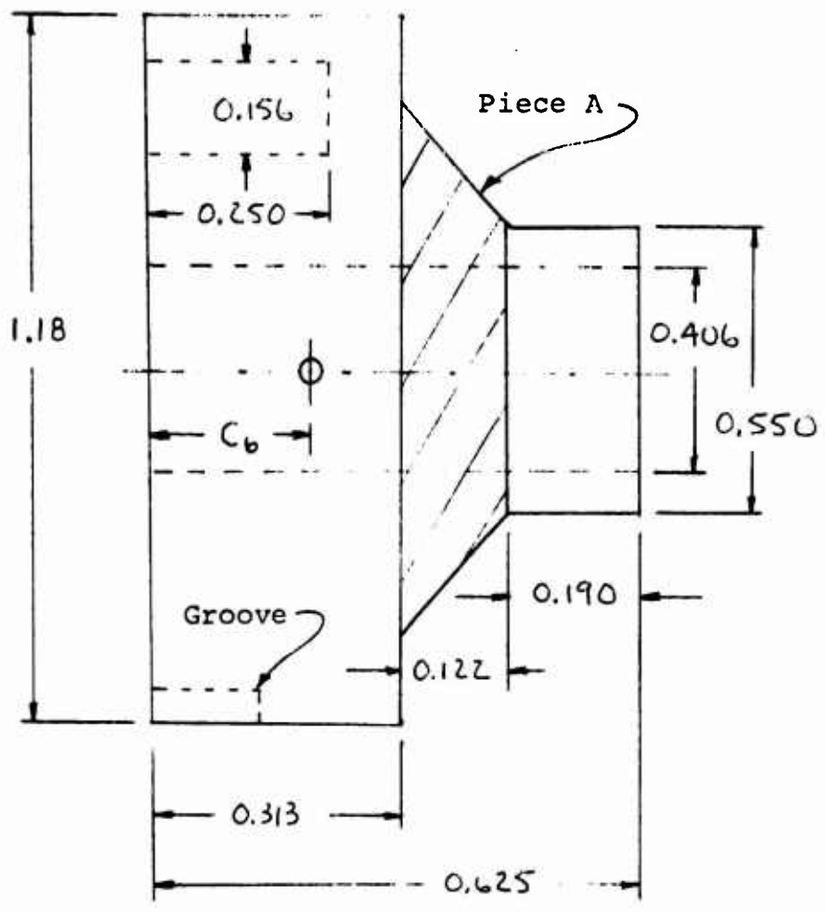

Figure A-1 - Inertia Weight

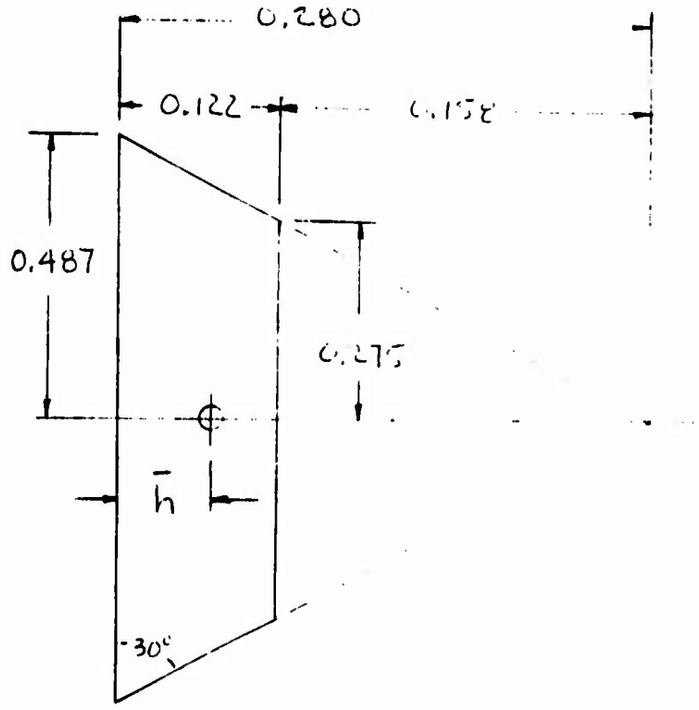

Figure A-2 - Piece A of Fig. A-1

For a right circular cone, the volume is $\frac{1}{3}\pi R^2 h$ and the centroid is at $h/4$.

The coordinate $\bar{h}$ is

Large Cone Small Dotted Cone

$$\bar{h} = \frac{\frac{1}{4}(0.280)\left[\frac{1}{3}\pi(0.487)^2(0.280)\right] - \left[0.122 + \frac{1}{4}(0.158)\right]\left[\frac{1}{3}\pi(0.275)^2(0.158)\right]}{\frac{1}{3}\pi(0.487)^2(0.280) - \frac{1}{3}\pi(0.275)^2(0.158)} \quad \text{(A-1)}$$

$$\bar{h} = \frac{0.00486 - 0.00202}{0.0695 - 0.0125} \quad \text{(A-2)}$$

$$\bar{h} = 0.0498 \quad \text{(A-3)}$$

The computation of C_6, the location of the centroid, is shown on the following page. The result is

$$C_6 = 0.181 \tag{A-4}$$

b. Moment of Inertia of The Inertia Weight About The Centroid

Figure A-3 shows the elements which comprise the inertia weight. The frustrum of a cone, Piece A, is approximated as a circular disc. For a right circular cylinder, the mass moment of inertia about a diameter through the centroid is $m(D^2/12 + \ell^2/12)$, where D is the diameter and ℓ is the height. The moment of inertia about an axis parallel to the centroidal diameter is

$$m\left[\frac{D^2}{12} + \frac{\ell^2}{12}\right] + m R_o^2 \tag{A-8}$$

where R_o is the distance between the two axes. From Figure A-3, I_o may be expressed as

$$I_o = I_{\oplus,1} + I_{\oplus,2} + I_{\oplus,3} + I_{\oplus,4} \tag{A-9}$$

The mass m may be written as γV, where γ is the mass density and V is the volume. I_o now appears as

$$\frac{I_o}{\gamma} = \frac{\pi(1.6)^2}{4}(0.313)\left[\frac{1.18^2}{16} + \frac{0.313^2}{12} + 0.024^2\right]$$

$$+ \frac{\pi(0.762)^2}{4}(0.122)\left[\frac{0.762^2}{16} + \frac{0.122^2}{12} + 0.193^2\right]$$

$$+ \frac{\pi(0.550)^2}{4}(0.190)\left[\frac{0.550^2}{16} + \frac{0.190^2}{12} + 0.349^2\right]$$

$$- \frac{\pi(0.406)^2}{4}(0.625)\left[\frac{0.406^2}{16} + \frac{0.625^2}{12} + 0.132^2\right] \tag{A-10}$$

$$C_6 = \frac{\frac{\pi(1.18)^2}{4}(0.313)\left(\frac{0.313}{2}\right) + 0.0125(0.313+0.0498) + \frac{\pi(0.550)^2}{4}(0.190)\left[0.313+0.122+\frac{0.190}{2}\right]}{\frac{\pi(1.18)^2}{4}(0.313) + 0.0125 + \frac{\pi(0.550)^2}{4}(0.190)}$$

$$\frac{-\frac{\pi(0.406)^2}{4}(0.625)\left(\frac{0.625}{2}\right) - 3\left\{\pi\frac{(0.156)^2}{4}(0.250)\left(\frac{0.250}{2}\right)\right\}}{-\pi\frac{(0.406)^2}{4}(0.625) - 3\left\{\pi\frac{(0.156)^2}{4}(0.250)\right\}} \qquad \text{(A-5)}$$

$$C_6 = \frac{0.342(0.157)+0.0125(0.363)+0.045(0.530)-0.081(0.313)-0.0145(0.125)}{0.342+0.0125+0.045-0.081-0.0145} \qquad \text{(A-6)}$$

$$C_6 = \frac{0.0550}{0.304} = 0.181 \qquad \text{(A-7)}$$

$$\frac{I_o}{\gamma} = 0.0386 \tag{A-11}$$

Using a specific weight for aluminum of $0.1\ lb/in^3$,

$$I_o = \frac{0.1\ lb/in^3}{386\ in/sec^2}\ (0.0386\ in^5) \tag{A-12}$$

$$I_o = 1.00 \times 10^{-5}\ lb\ sec^2\ in \tag{A-13}$$

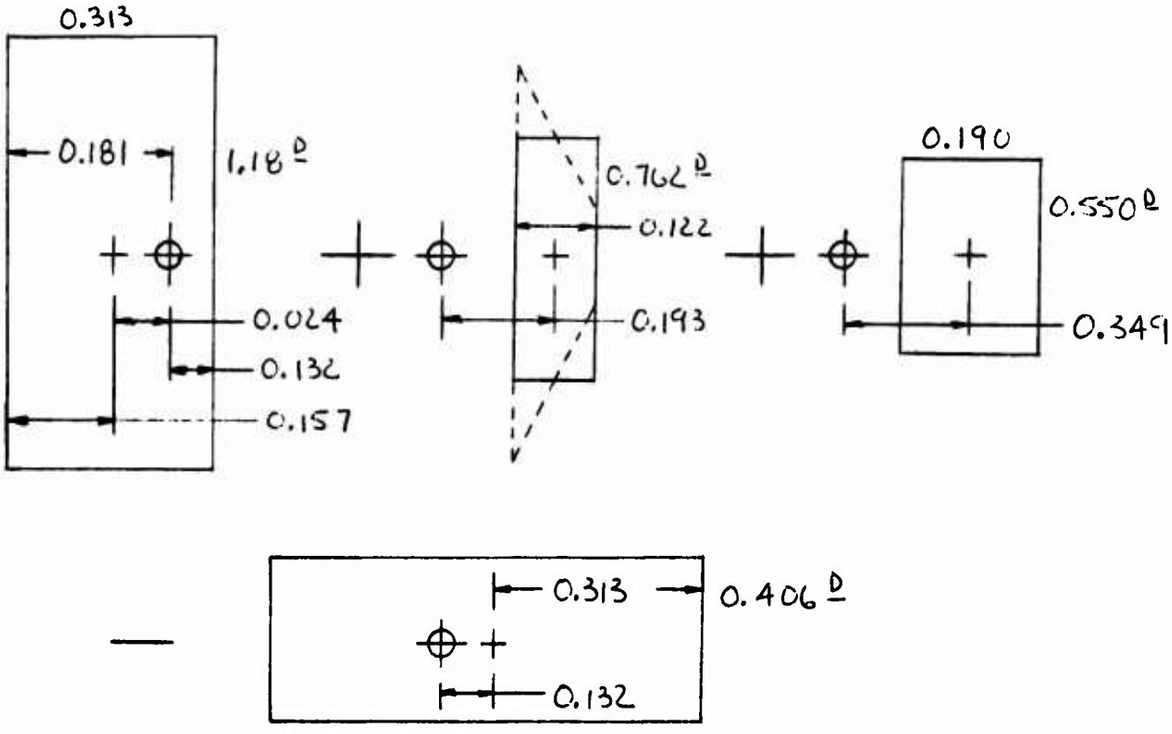

Figure A-3 - Subsections of Inertia Weight

C. Relationship of Inertia Weight Motion to Graze Ball Motion

Figure A-4 shows the kinematic relationships between the inertia weight and the ball. X is the position of the ball and X_o is the most outboard position. y is the position of the CM and y_o is the position which corresponds to X_o. From consideration of the triangle

$$\tan\Theta = \frac{y - y_o}{X_o - X} \tag{A-14}$$

so that

$$X = (-\cot\theta)\,y + (X_o + y_o \cot\theta) \qquad \text{(A-15)}$$

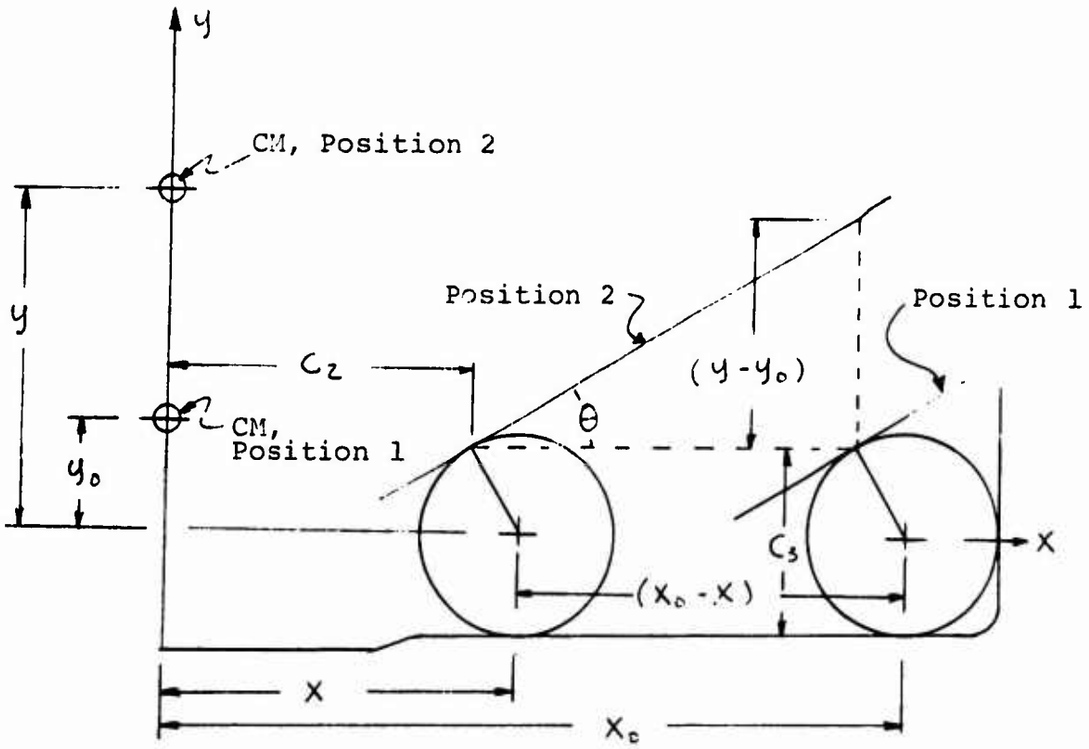

Figure A-4 Kinematic Relationship of Graze Ball and Inertia Weight

From Equation (6-13), (A-16)

$$X = C_8 y + C_9$$

Comparison of Equations (A-16) and (A-17) results in

$$C_8 = -\cot\theta \qquad \text{(A-17)}$$

$$C_9 = X_o + y_o \cot\theta \qquad \text{(A-18)}$$

d. Computation of Remaining Constants of The Problem

Figure A-5 shows the assembly of the inertia weight in the graze module housing. All of the dimensions shown are nominal. The ball diameter D is 5/16" , and the radius is 0.156 . From Figure A-5,

$$X_o = \frac{1.42}{2} - 0.156 = 0.554 \qquad \text{(A-19)}$$

$$0.171 + y_o + 0.181 = 0.625 \qquad \text{(A-20)}$$

$$y_o = 0.273 \qquad \text{(A-21)}$$

$$C_3 = 0.171 + 0.156 \cos 30^\circ = 0.171 + 0.156(0.866) \qquad \text{(A-22)}$$

$$C_3 = 0.306 \qquad \text{(A-23)}$$

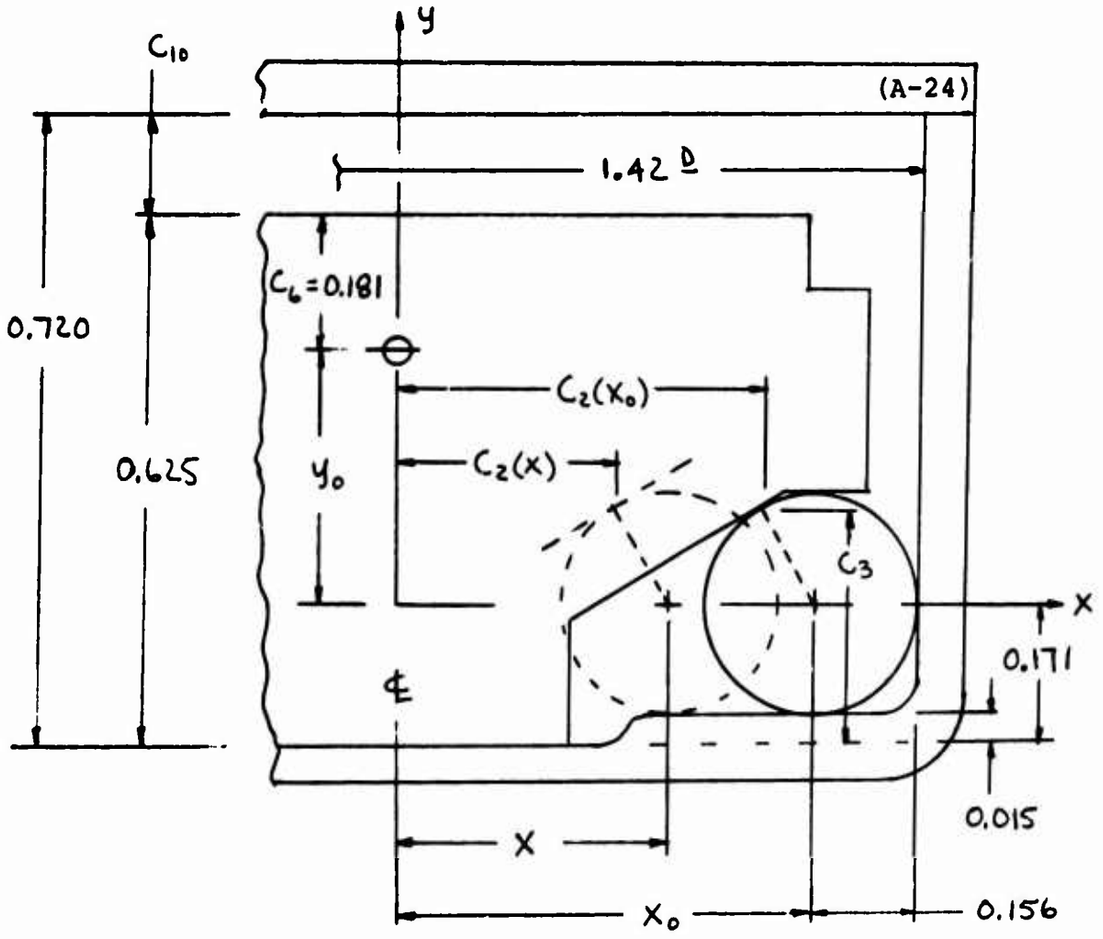

Figure A-5 - Geometry of Graze Ball Travel

The dimension C_{10} represents the maximum possible motion of the inertia weight with respect to the housing. From the figure,

$$C_{10} + 0.625 = 0.720 \qquad (A\text{-}24)$$

$$C_{10} = 0.095 \qquad (A\text{-}25)$$

The maximum displacement, $y_{MAX.}$, of the CM of the inertia weight is then

$$y_{MAX.} = y_0 + C_{10} \qquad (A\text{-}26)$$

$$= 0.273 + 0.095 \qquad (A\text{-}27)$$

$$y_{MAX.} = 0.368 \qquad (A\text{-}28)$$

The permissible range of y, the coordinate of the CM, is thus

$$y_0 \leq y \leq y_0 + C_{10} \qquad (A\text{-}29)$$

$$0.273 \leq y \leq 0.368 \qquad (A\text{-}30)$$

The dimension C_2 is a function of X. When $X = X_0$, $C_2 = C_2(X_0)$. For any other X, $C_2 = C_2(X)$. From the figure,

$$C_2 + D/2 \sin\theta = X \qquad (A\text{-}31)$$

$$C_2 + 0.156 \sin 30^\circ = X \qquad (A\text{-}32)$$

C_2 will now be found in terms of y. From Equation (A-15)

$$X = -y \cot\theta + X_0 + y_0 \cot\theta \qquad (A\text{-}33)$$

so that

$$C_2 = X_0 + y_0 \cot 30^\circ - 0.156 \sin 30^\circ - y \cot 30^\circ \qquad (A\text{-}34)$$

In this maximum outboard position, $y = y_0 = 0.273$,

so that

$$C_{2,MAX.} = X_0 + y_0 \cot 30^\circ - 0.156 \sin 30^\circ - y_0 \cot 30^\circ \qquad (A\text{-}35)$$

$$C_{2,MAX.} = 0.554 - 0.156(0.5) \qquad (A\text{-}36)$$

$$C_{2,MAX.} = 0.476 \qquad (A\text{-}37)$$

When the inertia weight touches the ceiling of the graze module housing, the displacement is given by Equation (A-28) and $C_{2,MIN.}$ is

$$C_{2,MIN} = 0.554 + 0.273(1.73) - 0.156(0.5) - 1.73(0.308) \quad (A-38)$$

$$C_{2,MIN.} = 0.313 \quad (A-39)$$

The possible range for C_2 in the present problem is then

$$0.313 \leq C_2 \leq 0.476 \quad (A-40)$$

e. Summary of Constants of Problem

The several constants of the problem are summarized below. The system of units is pound-seconds-inches.

$m_G = 1.08 \times 10^{-5}$ lb. sec.^{2}/in.

$m_I = 8.29 \times 10^{-5}$ "

$m_D = 5.18 \times 10^{-7}$ "

$m_F = 6.30 \times 10^{-6}$ "

$C_1 = 0.625$	$C_6 = 0.181$
$C_{2,MIN.} = 0.313$	$C_7 = 0.319$
$C_{2,MAX.} = 0.476$	$C_8 = -1.73$
$C_3 = 0.306$	$C_9 = 1.03$
$C_4 = 0.203$	$C_{10} = 0.095$
$C_5 = 0.444$	$C_{11} = 0.549$

$C_{12} = 0.040$	$\mu = 0.1$
$\theta = 30°$	$X_o = 0.554$
$\beta = 30°$	$y_o = 0.273$
$\tan\theta = 0.577$	$X_{01} = 0.140$
$\cot\theta = 1.73$	$y_{01} = 0.340$
$I_o = 1 \times 10^{-5}$ lb. sec^2. in.	$K = 18$ lb./in.
$F_q = 8.52$ (Maximum)	$K_o = 6$ lb./in.
$F_o = 3.9$ (Minimum)	$\pi = 0.063$
$y_{MAX.} = 0.368$	$D = 0.313$

The spin velocity is assumed to be for the 105 mm. Howitzer, M1, so that

$$\omega_y = 15{,}700 \text{ RPM} = 1{,}640 \text{ rad./sec.}$$

APPENDIX B - COMPARISON OF THE EQUATIONS OF MOTION OF THE INERTIA WEIGHT FOR $C_2 = C_{2,MIN.}$ AND $C_2 = C_{2,MAX.}$

The equations of motion of the inertia weight for the two regimes of operations, Equations (8-11) and (8-23), will now be evaluated for the two extreme valves of C_2. It will be seen that the differences in these equations which result from this variation in the magnitude of C_2 are small.

a. Both Primary and Secondary Balls Exert Wedging Effect on The Inertia Weight, Case I Operation

Using the numerical values in Appendix A, the equation of motion of the inertia weight, Equation (8-11), appears as

$$1.69 \times 10^{-4} \ddot{y} - 2.12 y = 3.64 \times 10^{-5} a_T + 1.37 \times 10^{-4} a_A$$

$$-3.2 \times 10^{-6} \alpha - 141 \qquad C_2 = C_{2,MAX.} = 0.476 \qquad \text{(B-1)}$$

$$1.73 \times 10^{-4} \ddot{y} - 222 y = 3.81 \times 10^{-5} a_T + 1.37 \times 10^{-4} a_A$$

$$-3.2 \times 10^{-6} \alpha - 147 \qquad C_2 = C_{2,MIN.} = 0.313 \qquad \text{(B-2)}$$

The above two equations will be compared term by term using a percent difference, %D, as defined below.

$$\%D = \frac{\text{Coefficient of Equation (B-2)} - \text{Coefficient of Equation (B-1)}}{\text{Coefficient of Equation (B-1)}}$$

The results are tabulated in Table B-1

Term	$\ddot{y}$	y	a_T	a_A	α	Const.
%D	+2.4	+4.7	+4.7	0	0	+4.3

Table B-1

b. Primary Ball Alone Exerts Wedging Effect on Inertia Weight, Case II Operation

The equations of motion of the inertia weight, Equation (8-23), for the two extreme valves of C_2 now appear as

$$1.10 \times 10^{-4}\ddot{y} - 56.2y = 1.39 \times 10^{-5} a_T + 1.39 \times 10^{-4} a_A$$

$$-3.2 \times 10^{-6}\alpha - 47.1 \qquad C_2 = C_{2,MAX.} = 0.476 \quad \text{(B-4)}$$

$$1.12 \times 10^{-4}\ddot{y} - 60.6y = 1.39 \times 10^{-5} a_T + 1.39 \times 10^{-4} a_A$$

$$-3.2 \times 10^{-6}\alpha - 50.4 \qquad C_2 = C_{2,MIN} = 0.313 \quad \text{(B-5)}$$

The percent differences, %D, in the above two equations are defined by Equation (B-6) as

$$\%D = \frac{\text{Coefficient of Equation (B-5)} - \text{Coefficient of Equation (B-4)}}{\text{Coefficient of Equation (B-4)}}$$

The results are tabulated in Table B-2

Term	$\ddot{y}$	y	a_T	a_A	α	Const.
% D	+1.8	+7.8	+7.8	0	0	+5.7

Table B-2

APPENDIX C - IMPACT OF INERTIA WEIGHT ON CEILING OF GRAZE MODULE

For very large magnitudes of the graze forcing functions, it is possible that the inertia weight might rebound off the ceiling of the graze with sufficient velocity to "pinch" a detent balls on their way out, and thus prevent the closing of the firing pin. This section establishes the conditions for the impact of the inertia weight on the ceiling of the graze module. The time t_3 is defined as the time when the inertia weight strikes the ceiling of the graze module housing. Since the mass of the inertia weight is much less than the mass of the shell, it will be assumed that the velocity of the shell is unaffected by this impact. Thus, the rebound velocity of the inertia weight will be governed by the definition of the coefficient of restitution.

For two spheres in direct central impact, the coefficient of restitution e is defined to be

$$e = \frac{V_B' - V_A'}{V_A - V_B} \tag{C-1}$$

where A and B signify the two spheres and the primes designate conditions after impact. The velocities in Equation (C-1) are absolute. The impact of the inertia weightwill be considered to be comparable to the case of spheres impacting, and a representative value of e will subsequently be chosen.

Figure C-1 shows the inertia weight and graze module ceiling, before impact. The velocity of the xyz coordinate system is V_B so that

$$V_A = V_B + \dot{y} \tag{C-2}$$

In view of the assumption,

$$V_B' \doteq V_B \tag{C-3}$$

and thus

$$V_A' = V_B' + \dot{y}' = V_B + \dot{y}' \tag{C-4}$$

where $\dot{y}'$ is the relative velocity of the inertia weight after impact.

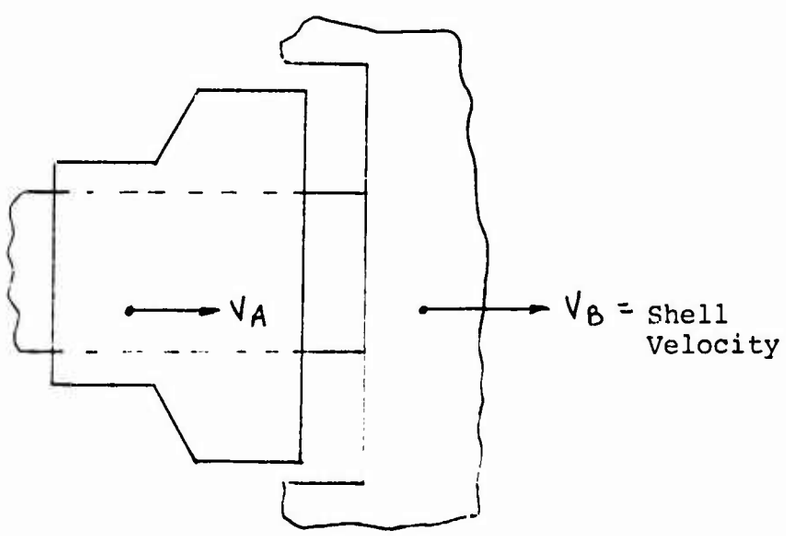

Figure C-1 - Inertia Weight

The results are substituted into Equation (C-1), with the result

$$e = \frac{V_B' - V_A'}{V_A - V_B} = \frac{V_B - (V_B + \dot{y}')}{(V_B + \dot{y}) - V_B} \tag{C-5}$$

$$e = -\frac{\dot{y}'}{\dot{y}} \tag{C-6}$$

The final result is

$$\dot{y}' = -e\,\dot{y}$$

The boundary conditions at $t = t_3$ are then

$$t = t_3 \qquad y = y_{MAX.} \tag{C-8}$$

$$t = t_3 \qquad \dot{y}\Big|_{t_3^+} = -e\,\dot{y}\Big|_{t_3^-} \tag{C-9}$$

where $y_{MAX.}$ is the maximum displacement of the CM of the inertia weight.

APPENDIX D - NOMENCLATURE

Term		Definition (Page on which first used)
d	—	Shell Dimension (12)
ℓ	—	Shell Dimension (12)
a_A	—	Component of shell acceleration (12)
a_N	—	Component of shell acceleration (12)
x	—	Component of shell acceleration (12)
P_A	—	Axial component of graze force (12)
P_N	—	Normal component of graze force (12)

Term	Definition (Page on which first used)
ζ —	Graze angle (12)
m —	Mass of shell (12)
I_{CM} —	Moment of inertia of shell about an axis normal to the longitudinal axis, with respect to center of mass (12)
a_T —	Lateral acceleration of graze module housing (12)
K_{CM} —	Radius of gyration of shell, about an axis normal to the longitudinal axis, with respect to the center of mass (13)
K_1 —	Constant of proportionality (13)
K_2 —	Constant of proportionality (13)
X_o, Y_o, Z_o —	Inertial coordinates (14)
X, Y, Z —	Secondary coordinates (14)
$\bar{a}_o$ —	Absolute acceleration of an arbitrary point (14)
P —	An arbitrary point (14)
$\ddot{\bar{R}}, \ddot{\bar{r}}, \frac{d\bar{\omega}}{dt}$ —	Terms in expression for absolute acceleration (15)
$\bar{I}, \bar{J}, \bar{K}$ —	Unit vectors in the X, Y, Z coordinate system (15)
$\bar{a}_{o,1}$ —	Absolute acceleration of primary graze ball (15)
ω_y —	Spin angular velocity of shell (15)
$\bar{a}_{o,2}$ —	Absolute acceleration of secondary graze ball (17)
θ —	Ramp angle of inertia weight (18)
$\bar{F}_{o,1}$ —	Reaction force on primary graze ball 1, by floor of graze module (18)
$\bar{F}_{1,1}$ —	Normal contact force between inertia weight and primary graze ball (18)
$F_{1x,1}, F_{1y,1}$ —	X and Y components of $\bar{F}_{1,1}$ (19)
m_G —	Graze ball mass (20)
C_x —	Constant (21)
C_y —	Constant (21)

Term	Definition (Page on which first used)
$F_{I,2}$	— Normal contact force between inertia weight and secondary graze ball 2 (21)
$F_{Ix,2}$, $F_{Iy,2}$	— x and y components of $F_{I,2}$ (21)
$F_{y,3}$	— Direct axial force on inertia weight (21)
$F_{6,2}$	— Reaction force on secondary graze ball 2, by floor of graze module (22)
t_o	— Limiting time at which secondary balls no longer exert wedging action on inertia weight (23)
$\bar{a}_{o,I}$	— Absolute acceleration of inertia weight (26)
F_2 , F_5	— Normal reactions on inertia weight (27)
F_3 , F_4	— Friction forces induced by F_2 and F_5 (27)
μ	— Constant coefficient of friction (30)
F_7	— Inertia force of inertia weight (27)
F_8	— Total force of three inertia weight creep springs (27)
K	— Total spring constant of three inertia weight creep springs (27)
F_9	— Total initial force of three inertia weight creep springs (27)
I_o	— Mass moment of inertia of inertia weight, about an axis through the center of mass and normal to the longitudinal axis (27)
m_I	— Inertia weight mass (27)
$C_1, C_2, C_3, C_4, C_5, C_6, C_7$	— Constants (28)
$F_{F,TOT.}$	— Total axial friction force on inertia weight (31)
$A_1, A_2, A_3, A_4, A_5, A_6$	— Constants (36)
y_o	— Initial displacement, at $t = 0$, of center of mass of inertia weight (36)
a_{l_o}	— Peak magnitude of triangular approximation of graze module lateral acceleration (38)
t_1	— Time which corresponds to a_{l_o} (38)
t_2	— Time of cessation of triangular approximation of graze module lateral acceleration (38)

Term	Definition (Page on which first used)
K_5	Constant (42)
K_6	Constant (43)
y_1	Axial displacement of firing pin (51)
y_{01}	Positive constant (51)
x_1	Radial displacement of detent ball (51)
x_{01}	Positive constant (51)
r	Radius of detent ball (52)
β	Ramp angle of firing pin (52)
φ	Variable angle (52)
φ_0	Maximum value of φ (54)
$P_{1,3}$, $P_{1,4}$	Normal contact forces between firing pin and detent balls (55)
$P_{2,3}$, $P_{2,4}$	Reaction forces, in the axial direction, on detent balls (55)
ℓ	Free length of firing pin spring (55)
K_0	Spring constant of firing pin spring (55)
F_s	Force of firing pin spring (55)
F_0	Initial force, at $t = 0$, of firing pin spring (55)
m_D	Mass of detent ball (57)
m_F	Mass of firing pin (57)
C_{11}	Constant (63)
A, B, C, D	Designation of cases of combined motion of inertia weight, detent balls and firing pin (54)
C_{12}	Constant (65)
t_4	Time at which inertia weight loses contact with detent balls (67)
t_5	Time at which inertia weight impacts on ceiling of graze module housing (95)

Term	Definition (Page on which first used)
y_A ——	Constant value of y (69)
y_B ——	Constant value of y (70)
y_C, y_D ——	Variable values of y (70)
y_E ——	Constant value of y (70)
j ——	Dummy subscript to represent A,B or E (72)
x_i^B ——	x_i motion for Case B Operation (73)
t_5 ——	Time at which detent balls lose contact with firing pin (74)
y_i^D ——	y_i motion for Case D Operation (74)
$y_{i,MAX.}$ —	Maximum displacement of firing pin (75)
t_6 ——	Time at which firing pin achieves its maximum displacement (75)
t_7 ——	Time at which detent balls have moved through the distance C_{10} (75)
y_i^E ——	Motion of firing pin for $t > t_7$ (76)
$X_{i,a}(t)$ —	Certain function of X_i (66)
$X_{i,b}(t)$ —	Certain function of X_i (66)
X_c ——	Maximum outward displacement of graze balls (88)
C_{10} ——	Maximum relative displacement of inertia weight with respect to graze module housing (91)
$y_{MAX.}$ —	Maximum displacement of CM of inertia weight (91)
D ——	Diameter of graze balls (90)
e ——	Coefficient of restitution (96)
V_B ——	Absolute velocity, before impact, of the coordinate system (96)
V_A ——	Absolute velocity, before impact, of the inertia weight (96)
V_i' ——	Absolute velocity, after impact, of the coordinate system (96)

Term		Definition (Page on which first used)
K_3	——	Constant (39)
K_4	——	Constant (39)
y_c	——	Complementary solution for y (40)
y_p	——	Particular solution for y (40)
V_A'	——	Absolute velocity, after impact, of the inertia weight (96)
t_ϕ	——	Time for the center of a graze ball to rotate 45° with respect to the shell axis. (77)

The reference for dimensions used in this report is drawing KD-84300, entitled "Graze Delay Assembly." All of the other subassembly drawing numbers are included on this drawing.